Journal Pre-proof

Design, Synthesis, and Bioevaluation of Pyrazolo[1,5-*a*]Pyrimidine Derivatives as Tubulin Polymerization Inhibitors Targeting the Colchicine Binding Site with Potent Anticancer Activities

Gang Li, Yuxi Wang, Ling Li, Yichan Ren, Xin Deng, Jin Liu, Wei Wang, Meihua Luo, Shuwen Liu, Jianjun Chen

PII: S0223-5234(20)30491-8

DOI: https://doi.org/10.1016/j.ejmech.2020.112519

Reference: EJMECH 112519

To appear in: *European Journal of Medicinal Chemistry*

Received Date: 31 March 2020

Revised Date: 21 May 2020

Accepted Date: 29 May 2020

Please cite this article as: G. Li, Y. Wang, L. Li, Y. Ren, X. Deng, J. Liu, W. Wang, M. Luo, S. Liu, J. Chen, Design, Synthesis, and Bioevaluation of Pyrazolo[1,5-*a*]Pyrimidine Derivatives as Tubulin Polymerization Inhibitors Targeting the Colchicine Binding Site with Potent Anticancer Activities, *European Journal of Medicinal Chemistry*, https://doi.org/10.1016/j.ejmech.2020.112519.

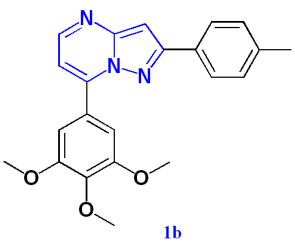

1b

Average IC_{50}: 28.0 nM

HLM $t_{1/2}$=125 min

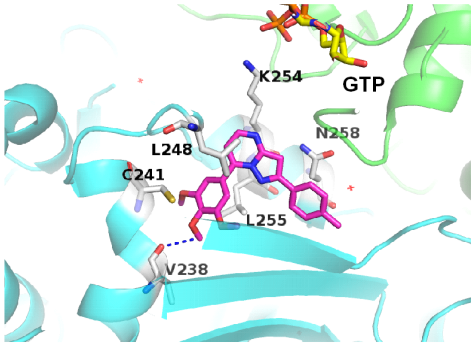

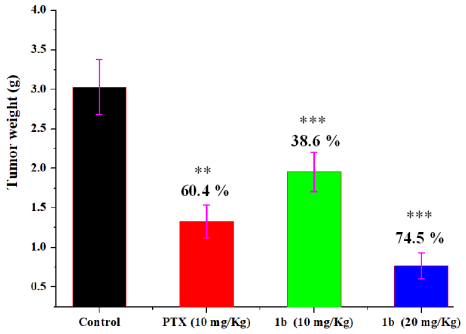

Design, Synthesis, and Bioevaluation of Pyrazolo[1,5-*a*]Pyrimidine Derivatives as Tubulin Polymerization Inhibitors Targeting the Colchicine Binding Site with Potent Anticancer Activities

Gang Li[1], *Yuxi Wang*[2], *Ling Li*[3], *Yichan Ren*[3], *Xin Deng*[3], *Jin Liu*[3], *Wei Wang*[3], *Meihua Luo*[1], *Shuwen Liu*[3], *Jianjun Chen*[3*]

[1]Department of oncology, Shunde Hospital, Southern Medical University (The First People's Hospital of Shunde), Foshan, 528300, China

[2]State Key Laboratory of Biotherapy and Cancer Center, West China Hospital, Sichuan University, and Collaborative Innovation, Center of Biotherapy, Chengdu, Sichuan 610041, China

[3]School of Pharmaceutical Sciences, Guangdong Provincial Key Laboratory of New Drug Screening, Southern Medical University, Guangzhou 510515, China.

*Corresponding Author: Jianjun Chen. School of Pharmaceutical Sciences, Guangdong Provincial Key Laboratory of New Drug Screening, Southern Medical University, Guangzhou 510515, China. Email: jchen21@smu.edu.cn.

ABSTRACT

A series of Pyrazolo[1,5-*a*]Pyrimidine analogues were designed and synthesized as novel tubulin inhibitors. Among them, compounds **1a** and **1b** showed the highest antiproliferative activity against a panel of cancer cell lines with average IC_{50} values of 24.8 nM and 28 nM, respectively. We determined the crystal structures of **1a** and **1b** in

complex with tubulin and confirmed their direct binding to the colchicine site. Compounds **1a** and **1b** also effectively inhibited tubulin polymerization *in vitro*, induced cell cycle arrest in G2/M phase, and inhibited cancer cell migration. In addition, compound **1b** exhibited high metabolic stability in human liver microsomes. Finally, **1b** was highly effective in suppressing tumor growth in a B16-F10 mouse melanoma model without apparent toxicity. In summary, these results suggest that **1b** represents a promising tubulin inhibitor worthy of further investigation.

Keywords: Tubulin inhibitor, Colchicine binding site, Pyrazolo[1,5-*a*]pyrimidine, Antitumor

1. Introduction

Microtubules are composed of α-tubulin and β-tubulin, which are the key components of cytoskeleton[1-3]. Due to the critical role of microtubules in mitosis, maintenance of cellular shape, and intracellular transport, microtubules are regarded as an excellent target for anticancer therapeutic agents such as microtubule targeting agents (MTAs). MTAs (e.g. paclitaxel, vinblastine and colchicine) interfere with the dynamic equilibrium of tubulin/microtubule through the well-known six binding sites[4] (taxane, vinca, laulimalide, maytansine, pironetin and colchicine sites), which could lead to cell cycle arrest and limit cell proliferation thus resulting in cell death[5-7]. MTAs can be divided into two classes: microtubule stabilizers (e.g. taxanes) and microtubule destabilizers (vinca alkaloids and colchicine). Current available MTAs such as paclitaxel,

vincristine, and vinblastine bind to the taxanes or vinca alkaloids sites in tubulin and have enjoyed considerable clinical success, however, the further application of these MTAs is often hampered by several drawbacks including low water solubility and the development of multidrug resistance[8-10]. During the last 10 years, the search for MTAs that can potentially overcome the above disadvantages has been intensified, and extensive research suggest that colchicine binding site inhibitors (CBSIs) may provide better clinical outcomes compare to other MTAs such as taxanes[11-13].

We have previously developed several series of CBSIs including SMART (4-substituted methoxybenzoyl-aryl-thiazoles)[14], ABI (2-aryl-4-benzoyl-imidazoles)[15, 16] and SAI (substituted-2-aryl imidazoles) analogues[17], which showed potent *in vitro* antiproliferative activities with IC_{50} in the nanomolar range and high *in vivo* antitumor efficacy, more importantly, they could effectively overcome P-gp mediated MDR (multi-drug resistance). Despite the favorable pharmacodynamic profiles, the ABI and SMART analogs contain a metabolically labile carbonyl (ketone) group between the B-ring and C-ring (**Figure 1**), which is prone to metabolic reductions by human liver microsomes[18, 19]. In an effort to improve the metabolic stability, we designed a series of nonketones, namely, the ring-fused pyrazolo[1,5-*a*]pyrimidine analogues, by incorporating the carbonyl moiety into a six-membered pyrimidine ring, as the ring-fusion strategy is a common approach frequently applied in medicinal chemistry to improve the stability of a compound[20, 21]. We chose the pyrazolo[1,5-*a*]pyrimidine scaffold as the bioisostere of the B-ring and ketone of the SMART and ABI analogs,

because the pyrazole and pyrimidine groups are widely used templates in many drugs[22, 23]. While for the A-ring, we explored the indole group, substituted phenyl and other aromatic groups. The 3,4,5-trimethoxy phenyl (TMP) group was maintained as the C-ring of the target compounds because the TMP moiety is an important pharmacophoric feature for antitumor activity and has to be kept intact[24]. We herein describe the synthesis and biological evaluation of the novel nonketone tubulin inhibitors that contain the pyrazolo[1,5-*a*]pyrimidine moiety as potential anticancer agents.

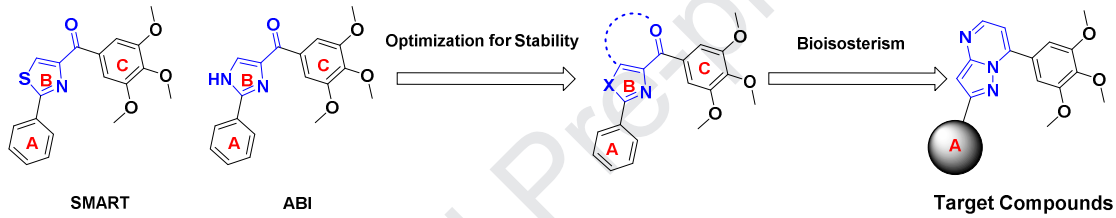

Figure 1. Design of target compounds by ring-fusion strategy

2. RESULTS AND DISCUSSION

2.1. Chemistry

Compounds **1a-y** and **1aa-af** were synthesized according to the synthetic route illustrated in **Scheme 1**. Firstly, 3,4,5-Trimethoxyacetophenone was condensed with *N*, *N*-dimethylformamide dimethyl acetal in DMF to afford intermediate **2**, followed by a ring closure reaction with 3-bromo-1*H*-pyrazol-5-amine to give the key intermediate **3**, then compound **3** was coupled with appropriate aryl boronic acids to generate compounds **1a-y**. The phenylsulfonyl group of compound **1y** was removed to produce compound **1aa.** Introduction of a methyl and a hydroxymethyl group to the *N*-1 position on the indole moiety of **1aa** provided compounds **1ab** and **1ac**, respectively. The conversion of

compound **1q** to **1ad** was achieved by reducing the 4-ethoxycarbonyl moiety in the presence of $LiAlH_4$. Compound **1ae** was prepared by methylating the indole *N*-1 position of **1c**. Compound **1af** was obtained by reducing the nitro group of compound **1h** with Pd/C under H_2 atmosphere.

Scheme 1. Synthesis of compounds **1a-y, 1aa-af, 4a-b** and **7**

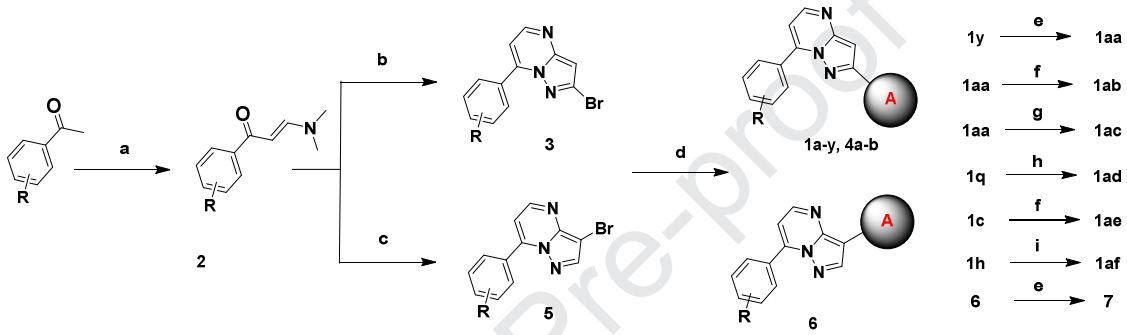

R = 3,4,5-trimethoxy

1a: A ring = 5-(1-methyl-*1H*-indole)
1b: A ring = 4-methyl-phenyl
1c: A ring = 6-indole
1d: A ring = 4-vinylphenyl
1e: A ring = 3,4-dimethyl-phenyl
1f: A ring = 4-*N*,*N*-dimethyl-phenyl
1g: A ring = phenyl
1h: A ring = 3-nitro-4-methoxy-phenyl
1i: A ring = 3-fluoro-4-methoxy-phenyl
1j: A ring = 4-methoxy-phenyl
1k: A ring = 3-(1-ethyl-carbazole)
1l: A ring = 5-(1-methyl-indazole)
1m: A ring = 3-methyl-phenyl
1n: A ring = 3,4,5-trimethoxy-phenyl
1o: A ring = 4-morpholinyl-phenyl
1p: A ring = 4-(1-methyl-pyrazole)
1q: A ring = 4-ethoxycarbonyl-phenyl
1r: A ring = 3-(1-Boc-indole)
1s: A ring = 4-fluoro-phenyl
1t: A ring = 3-cyano-phenyl
1u: A ring = 4-acetylphenyl
1v: A ring = 4-trifluoromethyl-phenyl
1w: A ring = 4-chloro-phenyl
1x: A ring = 4-tert-butyl-phenyl
1y: A ring = 3-(1-benzenesulfonyl chloride-*1H*-indole)
1aa: A ring = 3-indole
1ab: A ring = 3-(1-methyl-*1H*-indole)
1ac: A ring = 3-(1-methylol-*1H*-indole)
1ad: A ring = 4-methylol-phenyl
1ae: A ring = 6-(1-methyl-*1H*-indole)
1af: A ring = 3-amino-4-methoxy-phenyl
6: A ring = 3-(1-benzenesulfonyl chloride-*1H*-indole)
7: A ring = 3-indole

R = 4-fluoro

4a: A ring = 5-(1-methyl-*1H*-indole)
4b: A ring = 4-methyl-phenyl

Reagents and conditions: (a) *N*, *N*-dimethylformamide dimethyl acetal, DMF, 120 ^{o}C, 6h, 88.7%; (b) 3-bromo-1*H*-pyrazol-5-amine, AcOH, 80 ^{o}C, 8h, 93.3%; (c) 4-bromo-1*H*-pyrazol-5-amine, AcOH, 80 ^{o}C, 8h, 71.2%; (d) appropriate aryl boronic acid, $Pd(dppf)Cl_2$, Na_2CO_3 aq., DMF, 95 ^{o}C, 12h; (e) NaOH aq., EtOH, 50 ^{o}C, 8h; (f) NaH, dry THF, CH_3I, rt, 4h; (g) 37 % HCHO aq., 10 % NaOH, EtOH, 30 ^{o}C, 4h;(h) $LiAlH_4$, dry THF, rt, 4h; (i) Pd/C, H_2, CH_3OH/THF, rt, overnight.

The second series of compounds **7** and **4a-b** (A-ring as the 4-fluorophenyl group instead of 3,4,5-trimethoxyphenyl moiety) were obtained by a similar method shown in **Scheme 1**. Compound **11** (the positions of the indole group and 3,4,5-trimethoxy phenyl group were switched) was synthesized following the synthetic route outlined in **Scheme 2**. The 3-acetylindole was protected by the phenylsulfonyl group followed by a condensation reaction with *N*, *N*-dimethylformamide dimethyl acetal to give intermediate **9**. Compound **9** was cyclized with 3-bromo-1*H*-pyrazol-5-amine to provide the indazole intermediate **10**. Compound **10** was subject to a Suzuki coupling reaction with 3,4,5-trimethoxyphenylboronic acid followed by the deprotection of the phenylsulfonyl group to produce compound **11**.

Scheme 2. Synthesis of compound **11**

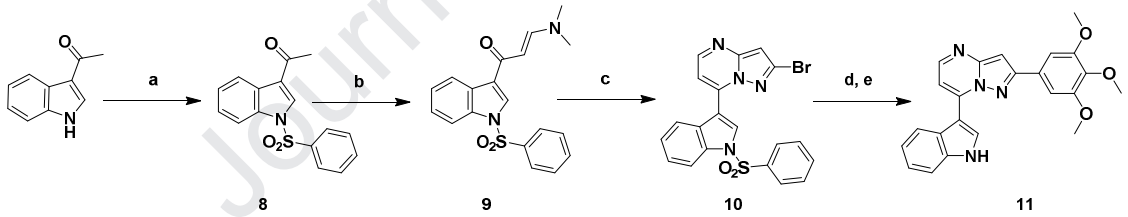

Reagents and conditions: (a) NaH, dry THF, benzenesulfonyl chloride, 25 ^{o}C, 6h, 87.2%; (b) *N*, *N*-dimethylformamide dimethyl acetal, DMF, 120 ^{o}C, 6h, 89.5%; (c) 3-bromo-1*H*-pyrazol-5-amine, CH_3COOH, 80 ^{o}C, 8h, 93.8 %; (d) 3,4,5-trimethoxyphenylboronic acid, $Pd(dppf)Cl_2$, Na_2CO_3 aq., DMF, 95 ^{o}C, 12 h, 76.8 %; (e) NaOH aq., EtOH, 50 ^{o}C, 8h, 70.2 %.

2.2. Biological evaluation

2.2.1 In vitro Antiproliferative Activity

The antiproliferative activities of the newly synthesized compounds were evaluated against five cancer cell lines (Hela, MCF-7, A549, HCT-116, B16-F10) using the CCK-8 assay with colchicine and paclitaxel as positive controls. In general, most of the pyrazolo[1,5-*a*]pyrimidine-based compounds (e.g. **1a-1g**, **1i-1l**) showed high antiproliferative activities with IC_{50} values in the nanomolar range (e.g. from 3 nM to 1 μM, **Table 1**). Compounds with electron-donating groups on the phenyl A-ring [e.g. **1b** (4-methylphenyl, average IC_{50} = 28 nM**)**, **1d** (4-vinyl, IC_{50} = 789 nM), **1e** (3,4-dimethyl, IC_{50} = 238 nM), **1f** (4-*N*,*N*-dimethyl, IC_{50} = 855 nM), **1j** (4-methoxy, IC_{50} = 536 nM), **1ad** (4-methylol, IC_{50} = 914 nM) and **1af** (3-amino-4-methoxy**,** IC_{50} = 157 nM)], displayed higher activities than the ones with electron-withdrawing groups [e.g. **1h** (3-nitro-4-methoxy, IC_{50} > 10 μM), **1i** (3-fluoro-4-methoxy, IC_{50} = 1.5 μM), **1q** (4-ethoxycarbonyl, IC_{50} > 10 μM), **1s** (4-fluoro, IC_{50} = 4.1 μM), **1t** (3-cyano, IC_{50} > 10 μM), **1w** (4-chloro, IC_{50} = 2.8 μM)], or the unsubstituted counterpart (**1g**, IC_{50} = 1.9 μM). Among them, compound **1b** (4-methylphenyl A-ring) exhibited the highest activity with an average IC_{50} value of 28 nM, which is comparable to that of paclitaxel (IC_{50} = 19.6 nM), and is slightly better than colchicine (IC_{50} = 67 nM). Replacing the 4-methyl group of **1b** with larger groups such as morpholinyl (**1o**, IC_{50} > 10 μM), acetyl (**1u**, IC_{50} = 3.9 μM), trifluoromethyl (**1v**, IC_{50} = 1.9 μM), and *t*-butyl (**1x**, IC_{50} > 10 μM), led to diminished activity. Compound **1n** with a 3,4,5-trimethoxypheny A-ring showed essentially a total loss of activity (IC_{50} > 10 μM). In addition to the phenyl A-ring, we also introduced an indole moiety as the A-ring, and explored the influence of the

positions of the indole moiety connecting to the central pyrazolo[1,5-*a*]pyrimidine ring on antiproliferative activities. For the N-methylated indole analogs (**1a**, **1ab**, **1ae**), the 5-indolyl compound **1a** showed better activity (IC_{50} = 24.8 nM) than the 3-indolyl analog **1ab** (IC_{50} = 556.6 nM) and the 6-indolyl analog **1ae** (IC_{50} value of 556.8 nM). For the 3-indolyl analogs, Compound **1aa** with no substitution on the indole NH (IC_{50} = 76.8 nM) and **1ac** with the N-methylol group (IC_{50} = 102 nM) displayed higher activity than **1ab** with the N-methyl group (IC_{50} = 556.6 nM).

Table 1 Anti-proliferative activities of compounds against five cancer cell lines[a].

Compound	IC_{50} (μM) [b]				
	Hela	MCF-7	A549	HCT-116	B16-F10
1a	**0.019 ± 0.001**	**0.003 ± 0.001**	**0.015 ± 0.001**	**0.039 ± 0.003**	**0.048 ± 0.004**
1b	**0.021 ± 0.001**	**0.047 ± 0.004**	**0.003 ± 0.001**	**0.048 ± 0.005**	**0.021 ± 0.002**
1c	0.125 ± 0.011	0.023 ± 0.003	0.170 ± 0.015	0.187 ± 0.016	0.055 ± 0.008
1d	0.882 ± 0.075	0.193 ± 0.027	1.029 ± 0.312	1.055 ± 0.389	0.788 ± 0.065
1e	0.241 ± 0.021	0.026 ± 0.003	0.272 ± 0.021	0.261 ± 0.019	0.391 ± 0.034
1f	0.378 ± 0.032	0.044 ± 0.003	1.103 ± 0.103	2.051 ± 0.197	0.702 ± 0.084
1g	0.458 ± 0.042	0.254 ± 0.021	0.208 ± 0.014	3.876 ± 0.331	4.734 ± 0.420
1h	>10	>10	>10	>10	>10
1i	0.236 ± 0.022	0.183 ± 0.010	0.545 ± 0.048	2.840 ± 0.232	3.952 ± 0.331
1j	0.373 ± 0.030	0.125 ± 0.011	0.376 ± 0.031	0.404 ± 0.038	1.405 ± 0.102

1k	0.160 ± 0.012	0.242 ± 0.021	0.643 ± 0.062	1.53 ± 0.096	1.805 ± 0.324
1l	0.097 ± 0.007	0.279 ± 0.023	0.233 ± 0.016	2.436 ± 0.212	1.473 ± 0.130
1m	4.226 ± 0.390	1.076 ± 0.092	5.731 ± 0.502	6.152 ± 0.562	2.220 ± 0.182
1n	>10	>10	>10	>10	>10
1o	>10	>10	>10	>10	>10
1p	1.831 ± 0.227	0.274 ± 0.026	1.147 ± 0.317	2.106 ± 0.282	1.238 ± 0.268
1q	>10	>10	>10	>10	>10
1r	3.768 ± 0.436	0.268 ± 0.021	2.065 ± 0.178	5.716 ± 0.530	3.070 ± 0.220
1s	5.836 ± 0.475	1.280 ± 0.094	3.797 ± 0. 352	5.033 ± 0.761	4.544 ± 0.402
1t	>10	>10	>10	>10	>10
1u	1.810 ± 0.105	5.229 ± 0.497	4.098 ± 0.386	4.394 ± 0.326	3.933 ± 0.321
1v	1.840 ± 0.179	2.444 ± 0.221	2.069 ± 0.184	1.862 ± 0.138	1.772 ± 0.158
1w	1.488 ± 0.125	2.321 ± 0.210	3.065 ± 0.285	3.335 ± 0.296	4.091 ± 0.385
1x	>10	>10	>10	>10	>10
1aa	0.195 ± 0.012	0.085 ± 0.007	0.029 ± 0.003	0.035 ± 0.004	0.040 ± 0.005
1ab	0.399 ± 0.035	0.095 ± 0.008	1.342 ± 0.106	0.762 ± 0.065	0.185 ± 0.013
1ac	0.103 ± 0.009	0.019 ± 0.003	0.167 ± 0.013	0.128 ± 0.010	0.093 ± 0.007
1ad	0.456 ± 0.038	1.067 ± 0.088	1.100 ± 0.101	0.861 ± 0.074	1.086 ± 0.119
1ae	0.187 ± 0.011	0.074 ± 0.006	0.829 ± 0.075	1.037 ± 0.097	0.657 ± 0.058
1af	0.283 ± 0.015	0.027 ± 0.003	0.138 ± 0.010	0.251 ± 0.015	0.088 ± 0.006

4a	5.211 ± 0.429	4.579 ± 0.338	3.518 ± 0.442	2.157 ± 0.184	4.784 ± 0.569
4b	>10	>10	>10	>10	>10
7	>10	>10	>10	>10	>10
11	>10	>10	>10	>10	>10
Colchicine	**0.081 ± 0.006**	**0.018 ± 0.001**	**0.107 ± 0.009**	**0.042 ± 0.004**	**0.087 ± 0.006**
PTX	**0.041 ± 0.005**	**0.004 ± 0.001**	**0.012 ± 0.001**	**0.020 ± 0.001**	**0.021 ± 0.002**

[a] Cells were treated with different concentrations of the compounds for 48 h. Cell viability was measured by the CCK8 assay as described in the Experimental Section.

[b] IC_{50}: the half maximal inhibitory concentration. IC_{50} values are indicated as the mean ± SD (standard error) of at least three independent experiments.

Compound **7** (**Table 1**) with a 3-indolyl moiety is essentially inactive (IC_{50} >10 μM) probably due to their "straight" conformation which is not preferred for binding to the colchicine binding site in tubulin as compared to the "bent" conformation of compound **1aa** (IC_{50} = 76.8 nM, **Figure 2**). Similar results were also observed by Zhang's Group[25].

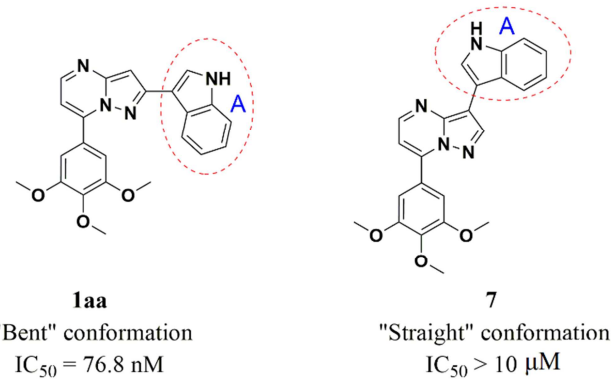

1aa
"Bent" conformation
IC_{50} = 76.8 nM

7
"Straight" conformation
IC_{50} > 10 μM

Figure 2. "Bent" and "Straight" conformations of target compounds.

In addition to the phenyl and indole A-ring, we also investigated other A-ring moieties, for example, 1-ethyl-carbazole (**1k**, IC_{50} = 876 nM), 1-methyl-indazole (**1l**, IC_{50} = 903 nM), and 1-methyl-pyrazole (**1p**, IC_{50} = 1.3 μM), these compounds displayed similar activity to that of **1f** (**(**IC_{50} = 855 nM**)**. The detailed Structure-Activity-Relationships (SARs) of this series of compounds are summarized in **Figure 3**.

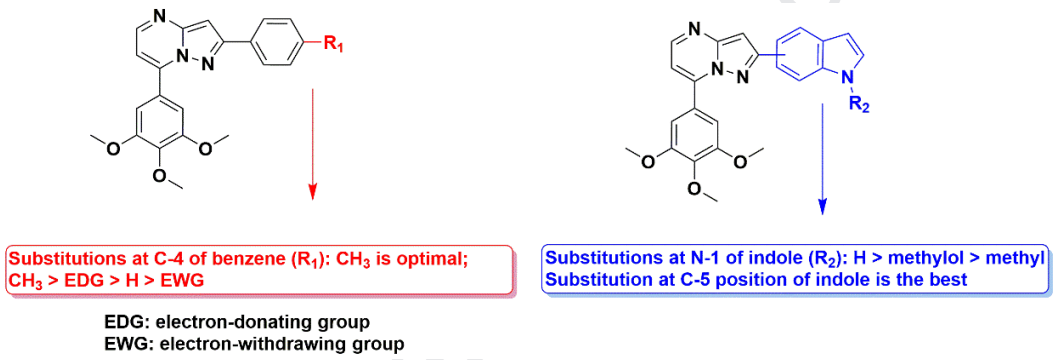

Figure 3. SARs of target compounds.

As a comparison, the compounds with a 4-fluorophenyl C-ring instead of a 3,4,5-trimethoxy phenyl C-ring displayed poor activity (IC_{50} of 4.0 μM and >10 μM for **4a** and 4**b**, respectively) than the corresponding 3,4,5-trimethoxy phenyl C-ring analogs **1a** and **1b** (IC_{50} of 24.8 nM and 28 nM for **1a** and **1b**, respectively, **Table 1**). These results suggest that the 3,4,5-trimethoxy C-ring is optimal for activity which is consistent with our previous findings[17, 24]. Compound **11** showed little or no activity (IC_{50} >10 μM) due to the switching of the positions of indole A-ring and 3,4,5- trimethoxy phenyl C-ring.

*2.2.2. Inhibitory effects of **1a** and **1b** on tubulin polymerization*

To understand the mechanism of action, we conducted a tubulin polymerization assay (at 37 ^{o}C without preincubation of tubulin with compounds) using the two most active compounds, **1a** and **1b**, along with colchicine and CA-4 as positive controls. As shown in **Figure 4**, the positive control compounds, colchicine and CA-4 inhibited tubulin polymerization with an IC_{50} of 7.5 μM and 1.1 μM (**Figure 4A**, **4B**), respectively; while compounds **1a** and **1b** inhibited tubulin polymerization with IC_{50} values of 6.7 μM (**Figure 4C**) and 2.1 μM (**Figure 4D**), respectively. It is well-known that the binding of colchicine to tubulin is slow, temperature-dependent and slowly reversible, therefore, we studied the effects of preincubation of tubulin with test compounds at different temperatures (e.g. 30, 37 ^{o}C) prior to the addition of GTP. As shown in **Figure S1** (supporting information), temperature has little effect on the binding of test compounds to tubulin [IC_{50} of 7.0, 6.4, 2.1 μM at 30 ^{o}C without preincubation (**Figure S1A, S1B, S1C**) vs 7.5, 6.7, 2.1 μM at 37 ^{o}C without preincubation (**Figure S1D, S1E, S1F**) for colchicine, **1a**, and **1b**, respectively]. While the preincubation of tubulin with compounds moderately increased the binding affinity of test compounds to tubulin [IC_{50} of 5.4, 5.7, 1.6 μM at 37 ^{o}C with 5 min preincubation (**Figure S1G, S1H, S1I**) vs 7.5, 6.7, 2.1 μM at 37 ^{o}C without preincubation (**Figure S1D, S1E, S1F**) for colchicine, **1a**, and **1b**, respectively].

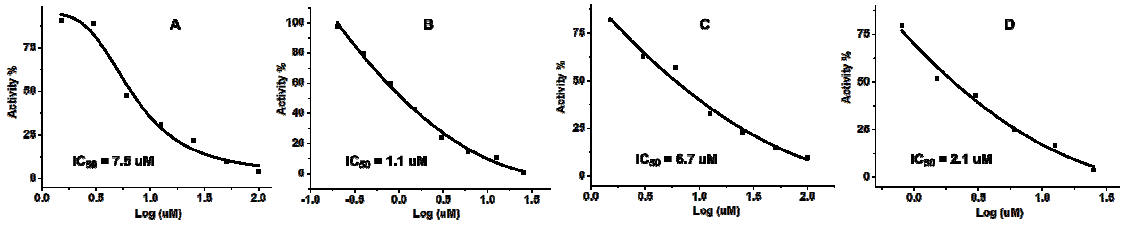

Figure 4. The inhibition of tubulin polymerization *in vitro* (at 37 ^{o}C without preincubation of tubulin with compounds) by colchicine (A), CA-4 (B), **1a** (C) and **1b** (D).

2.2.3. Cell Cycle Study by flow cytometry

Tubulin polymerization inhibitors are known to impact cell division, therefore, we evaluated the effects of the most potent compounds **1a** and **1b** on the cell cycle of MCF-7 cancer cells using flow cytometry. As shown in **Figure 5**, both **1a** and **1b** arrested cell cycle at G2/M phase in a dose-dependent manner. Compared with the control cells incubated with DMSO (**Figure 5A**), the incubation with colchicine (**Figure 5B**), **1a** (**Figure 5C, 5D**) and **1b** (**Figure 5E, 5F**) drastically increased the percentage of cells arrested in G2/M phase.

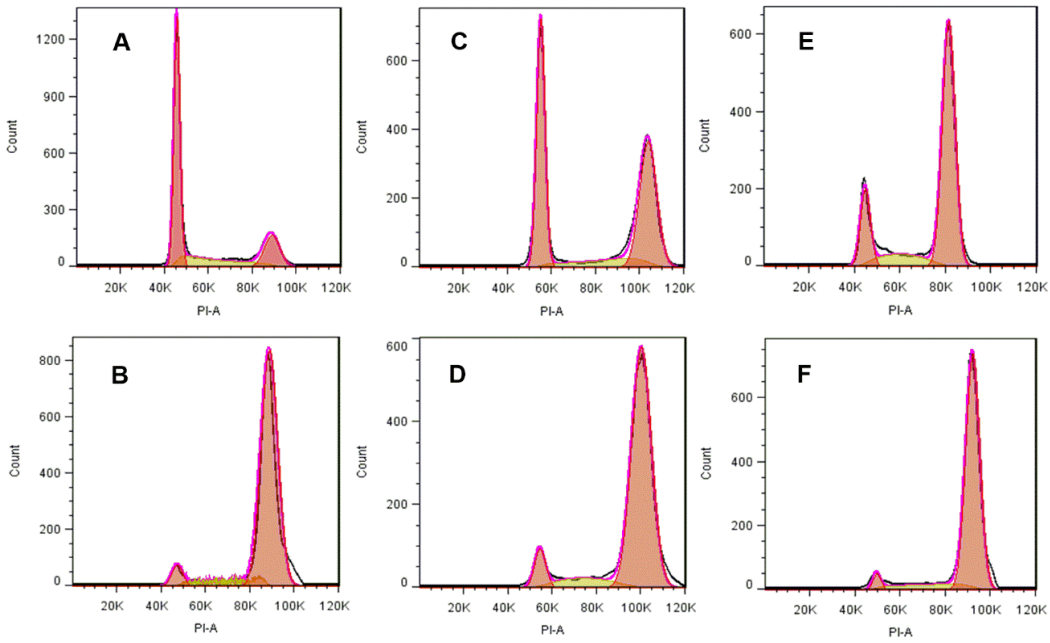

Figure 5. The cell cycle of MCF-7 cancer cells treated with **1a** and **1b**. (A) Vehicle control (DMSO); (B) colchicine, 10 nM; (C) **1a**, 5 nM; (D) **1a**, 10 nM; (E) **1b**, 5 nM; (F) **1b**, 10 nM.

2.2.4. Inhibition of Cancer Cell Migration

One of the important features of tumor cells is their ability to migrate to distant organs, leading to the formation of metastasized tumors. Our previous studies have shown that microtubule polymerization inhibitors are able to inhibit tumor metastasis[26], and similar results were also observed by other research groups [27, 28]. Therefore, we evaluated the effects of compound **1b** on cancer cell migration utilizing a wound healing assay. As shown in **Figure 6**, the wound closure was potently suppressed by **1b** in a dose-dependent manner, as compared to the control.

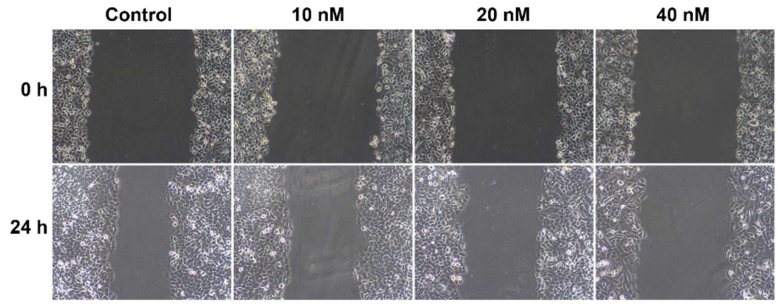

Figure 6. Effects of **1b** on MCF-7 cancer cell migration

2.2.5. Analysis of Immunofluorescence Staining

Microtuble dynamics play an essential role in cancer cell growth. To study whether compound **1b** is able to disrupt microtuble dynamics, we conducted an immunofluorescent assay in B16-F10 cells. As shown in **Figure 7**, the microtubule network in the control cells (DMSO, **Figure 7A**) exhibits normal arrangement and organization with the hair like, slim, and fibrous microtubules (green) wrapped around the cell nucleus (blue). Whereas in the PTX-treated cells (**Figure 7B**), the microtubules were stabilized as seen from the increased density of microtubules around the nuclei, which is consistent with PTX's mechanism of action as a microtubule stabilizer. For the cells treated with colchicine (160 nM, **Figure 7C**) or **1b** (40 nM, **Figure 7D**), the microtubules became short and wrapped around the nucleus in comparison with the control, indicating the disruption of microtubule network. These results suggest that **1b** could destabilize microtubule by inhibiting tubulin polymerization and disturbing microtubule networks, similar to colchicine and CA-4.

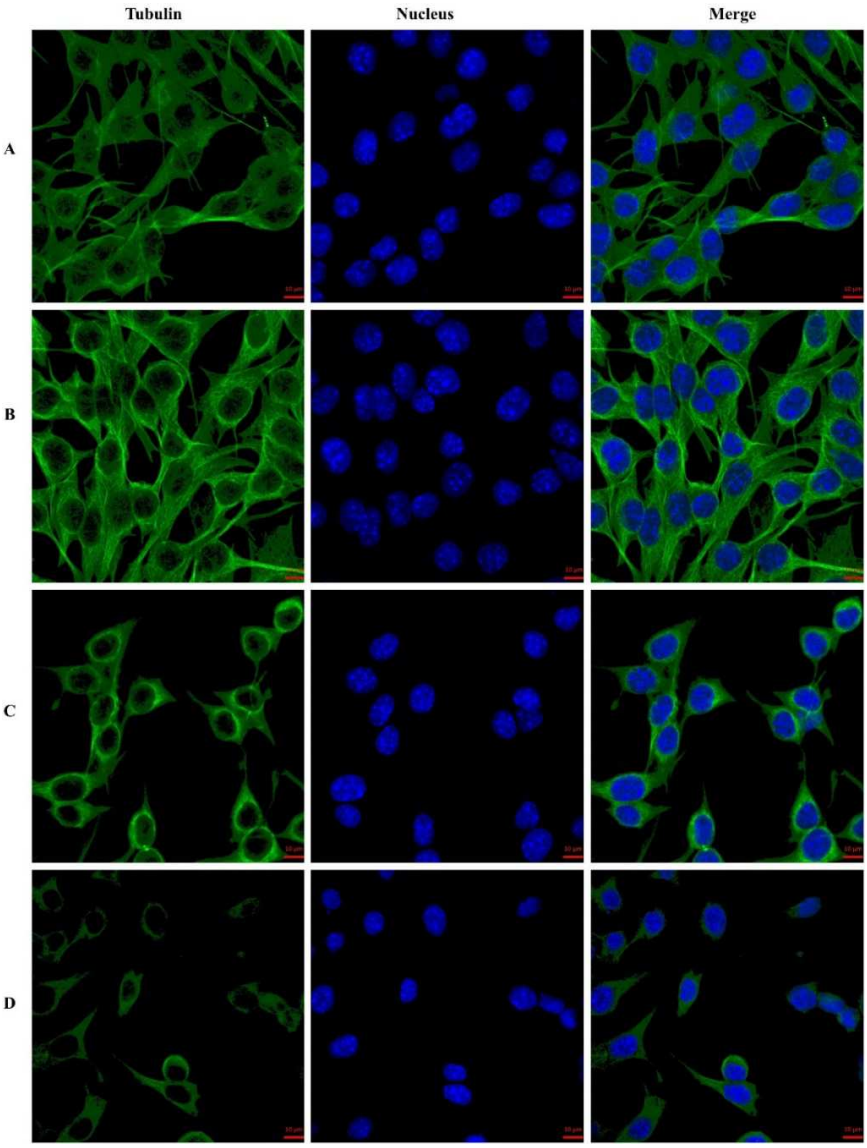

Figure 7. Effects of tested compounds on the cellular microtubule networks visualized by immunofluorescence microscopy. B16-F10 cells were treated with vehicle control 0.1% DMSO (A), PTX (40 nM) (B), Colchicine (160 nM) (C) and **1b** (40 nM) (D) for 6 h. Then, the cells were fixed and stained with anti-β-tubulin-FITC antibody (green), Alexa Fluor 488 dye and counterstained with DAPI (blue). The detection of the fixed and stained cells was performed by Carl Zeiss inverted microscope with plan-apochromat

63x/1.40 objective.

2.3 In vitro Metabolic Stability Studies

To test our hypothesis that the incorporation of the metabolically labile carbonyl linker into a cyclic structure could effectively block the metabolic reduction of the carbonyl group, thus prolonging the half-life of the compounds, we measured the metabolic stability for **1a** and **1b (**two of the most potent compounds) in human liver microsomes (HLM) and mouse liver microsomes (MLM). As shown in **Table 2**, compound **1b** exhibited significantly better metabolic stability in both HLM and MLM ($T_{1/2}$ = 125 and 120 min) than that of compound **1a** ($T_{1/2}$ = 20 min and 7 min) and the SMART compound ($T_{1/2}$ = 17 min and < 5min in HLM and MLM, respectively).

Table 2. Half-Lives of **1b** in liver microsomes of different species

Compounds	$T_{1/2}$ (min)	
	Human	mouse
1a	20 ± 1.2	7 ± 0.5
1b	125 ± 9.2	120 ± 8.0
SMART[20]	17	<5

*2.4. X-ray Structures of **1a** and **1b** in Complex with Tubulin*

To investigate the binding interactions of compounds with tubulin, we solved the crystal structures of compounds **1a** and **1b** in complex with T2R-TTL (composed of two α/β tubulin dimers, the stathmin-like protein RB3, and tubulin tyrosine ligase) (PDB code:

6LSN for **1a**, 6LSM for **1b**). The X-Ray/crystallographic data and structure refinement statistics are presented in **Table 3**.

Table 3. X-Ray data collection and refinement statistics.

	T_2R-TTL-1a (PDB code: 6LSN)	**T_2R-TTL-1b** (PDB code: 6LSM)
	Data collection	
Space Group	$P2_12_12_1$	$P2_12_12_1$
	Cell dimensions	
a, *b*, *c* (Å)	105.296, 158.458,181.959	105.553, 158.081,182.23
α, *β*, *γ* (°)	90, 90, 90	90, 90, 90
Resolution (Å)	50-2.45(2.49-2.45) [a]	30-2.75 (2.8-2.75) [a]
R_{merge} [b]	13.1(100.3)	0.129 (0.726)
$CC_{1/2}$ [c]	0.992(0.620)	0.997 (0.601)
$I/\delta(I)$	9.12(1.0)	12.8 (1.83)
Completeness (%)	100(99.8)	100 (100)
Redundancy	6.6(5.9)	11.4 (10.1)
	Structure refinement	
No. reflections	739524 (112697)	909059 (79742)
R_{work} / R_{free}	0.1789/0.2227	0.1813/0.2271
No. atoms	18041	17766
Protein	17448	17446
Ligand/ion	217	214
water	376	106
Average B factor	61.26	61.64
Protein	61.47	61.73
Ligand/ion	59	59
water	52.7	53.5
	R.m.s. deviations	
Bond lengths (Å)	0.01	0.01
Bond angle (°)	1.17	1.18
	Ramachandran plot	
Favored (%)	96.88	96.55
Allowed (%)	3.12	3.45
Outliers (%)	0	0

[a] Values in parentheses are for highest-resolution shell. [b] Rmerge as outlined by Diederichs and Karplus[29]. [c] CC1/2 is the Pearson correlation coefficient of two-half

data sets as described by Karplus and Diederichs[30].

As anticipated, compounds **1a** and **1b** are bound to the colchicine binding site of tubulin. The binding pocket is located at the interface of α- and β-tubulin, as opposed to the GTP molecule which occupies a pocket in the α-tubulin (**Figure 8A, 8D**). There are two water-bridged hydrogen bonds formed between **1a** and β-tubulin: the oxygen atom of the middle methoxy from the TMP (3,4,5-trimethoxyphenyl) moiety of **1a** with the -NH in β-Cys241 and -C=O in β-Val238 (**Figure 8B** and **8C**). This water mediated hydrogen bonding was also observed in several other crystal structures of tubulin in complex with colchicine binding site inhibitors [31, 32]. As for **1b**, one hydrogen bond was formed between it and β-tubulin: the middle methoxy group of the TMP (3,4,5-trimethoxyphenyl) with the -C=O of Val238 (**Figure 8E** and **8F**). In addition, the pyrazolo[1,5-*a*]pyrimidine moiety of compounds **1a** and **1b** is firmly wrapped in the colchicine-binding site with the formation of a tight hydrophobic “sandwich” by the side-chains of β-Lys254, β-Leu255 and β-Asn258 from one side and that of β-Leu248 from the other side[32, 33].

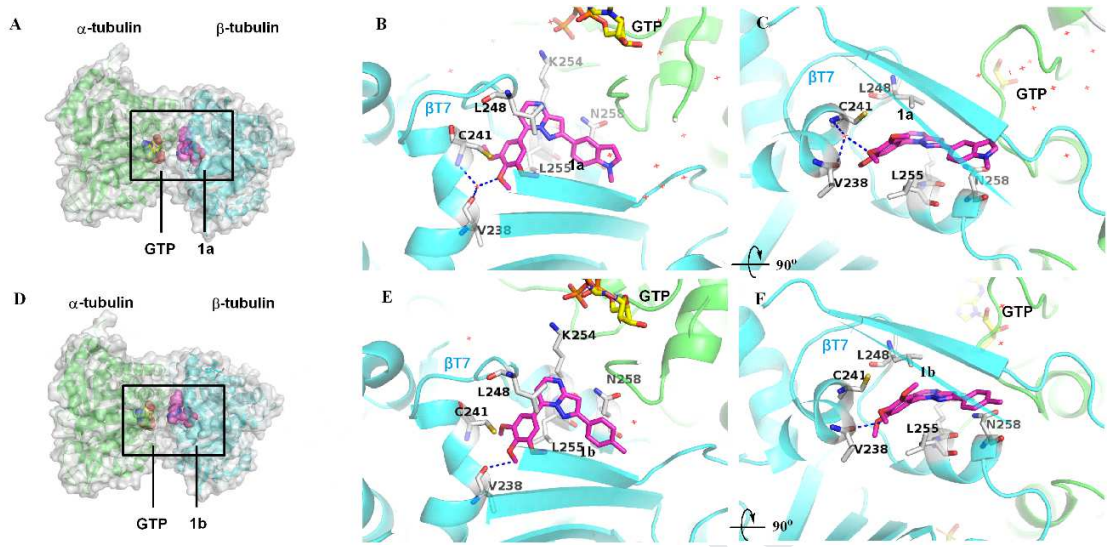

Figure 8. Complex structures of **1a** (6LSN) and **1b** (6LSM) with tubulin protein. (A, D) The overall structures of two compounds (**1a** and **1b**) in complex with tubulin. Colored in light green is the α units of T2R-TTL complex while colored in cyan is the β units; GTP and compounds **1a** and **1b** are shown in yellow and pink spheres, respectively. (B, E) Detailed interactions between **1a**/**1b** and tubulin at the colchicine binding domain. (C, F) 90^{o} clockwise rotation of corresponding structures along x axis. Compound-interacting residues are presented as grey sticks in β-subunit of tubulin, and are labeled in black. Oxygen and nitrogen atoms are colored read and blue, respectively. Hydrogen bonds are indicated with blue dashed lines.

2.5. In vivo Antitumor Activity

Based on the high *in vitro* antiproliferative activity and excellent metabolic stability, compound **1b** was selected to evaluate the *in vivo* antitumor efficacy using a melanoma B16-F10 tumor model in C57/BL mice. Each mouse was injected subcutaneously with 0.2 million B16-F10 melanoma cells. When tumors reached ~100 mm^3 in volume and

were palpable, mice were randomized into control or treatment (**1b** and paclitaxel) groups, and treated by intraperitoneal injection of compound **1b** (10, 20 m/kg), paclitaxel (PTX, 10 m/kg), or a vehicle solution for 16 days. The tumor volume/size and body weights of the mice were monitored and recorded every other day. As shown in **Figure 9**, compound **1b** dose-dependently decreased tumor volume and tumor weight (**Figure 9A, 9B**). At the dose of 10 mg/kg, **1b** decreased the tumor volume and tumor weight by 40.1 % and 38.6 %, respectively; At the dose of 20 mg/kg, **1b** significantly decreased the tumor volume and tumor weight by 77.4 % and 74.5 %, respectively, which is better than that of PTX (63.8 % and 60.4 % for decreasing the tumor volume and tumor weight, respectively, at a dose of 10 mg/kg, **Figure 9C**). Moreover, no significant body weight loss was observed in any of the treatment groups during the experiment (**Figure 9D**).

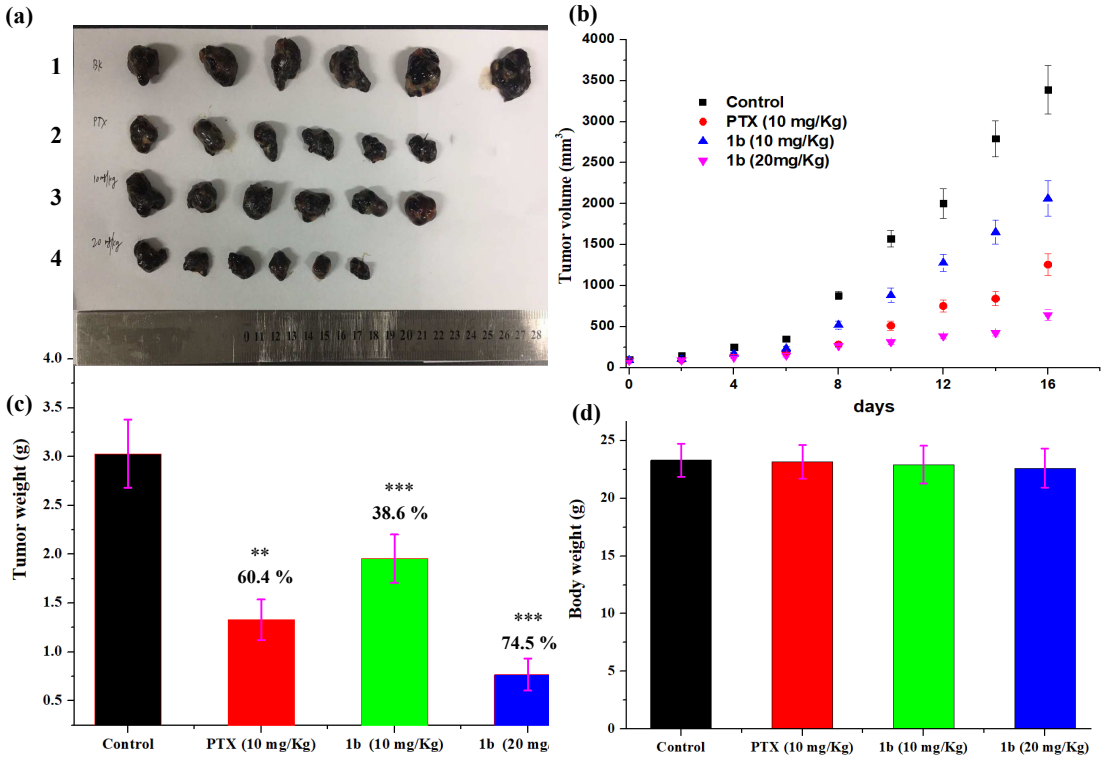

Figure 9. **1b** inhibits melanoma tumor growth *in vivo*. After administering vehicle (group 1), PTX (10 m/kg, group 2), **1b** (10 m/kg, group 3) and **1b** (20 m/kg, group 4) for 16 days, the mice were sacrificed, and tumors were excised and weighed. (a) The images of excised tumors in each group. (b) Changes of tumor volume during treatment. (c) Weight of the excised tumors of each group. (d) Changes of mice body weight during treatment. The data were presented as the mean ± SEM ** $P < 0.01$, ***$P < 0.001$, significantly different compared with the control by *t* test, n = 6.

In addition, pathohistological analysis utilizing H&E staining of the major organs (e.g. liver and kidney) collected at end of the *in vivo* study showed that there is no apparent organ-related toxicities (**Figure 10**). Overall, these data suggested that compound **1b** was highly efficacious in inhibiting melanoma tumor growth *in vivo* with

no obvious toxicity.

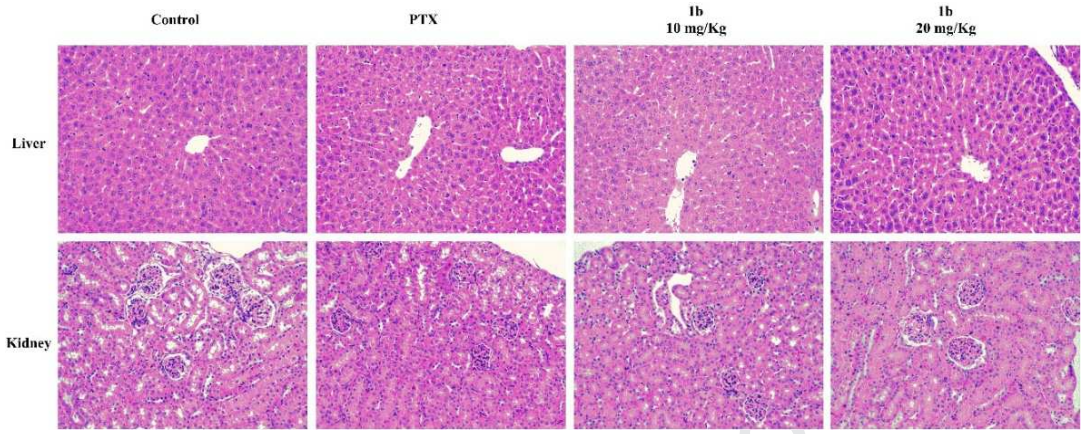

Figure 10. HE staining of major organs (liver and kidney) of mice. No abnormality or apparent toxicities were observed.

3. Conclusion

In summary, a series of pyrazolo[1,5-*a*]pyrimidine derivatives were designed and synthesized as tubulin polymerization inhibitors. Among them, compounds **1a** and **1b** exhibited the highest antiproliferative activities against five cancer cell lines *in vitro*. Further, compounds **1a** and **1b** were able to inhibit tubulin polymerization *in vitro* in a dose dependent manner. We also solved the high-resolution X-Ray crystal structure of compounds **1a** and **1b** in complex with tubulin, which confirmed the direct binding of **1a** and **1b** to the colchicine binding site in tubulin, validating the mode of action of **1a** and **1b** as tubulin inhibitors. Further mechanism studies indicated that **1a** and **1b** induced cell cycle arrest in G2/M phase, and inhibited cancer cell motility and migration. Importantly, **1b** exhibited excellent *in vitro* metabolic stability on human and mouse liver microsomes. Finally, **1b** was highly effective in suppressing tumor growth in a B16-F10 mouse

melanoma model without apparent toxicity. Taken together, these results suggest that compound **1b** represents a promising tubulin inhibitor deserving further investigation.

4. Experimental section

4.1. Chemistry

Unless otherwise noted, all chemicals/reagents were purchased from commercial suppliers and were used without further purification. The reference compounds colchicine and paclitaxel were purchased from InvivoChem (Libertyville, IL 60048, USA). Thin layer chromatography (TLC) analysis of reaction mixtures was performed on Dynamic adsorbents silica gel F-254 TLC plates with fluorescent indicator visualized at 254 nm and 365 nm. Column chromatography for purification of compounds was performed on silica gel (200-300 mesh). ^{1}H NMR (400 MHz) and ^{13}C NMR (100 MHz) spectra were recorded with a Bruker AVANCE 400MHz spectrometer. Chemical shifts were reported in ppm units (parts per million) and all coupling constants (*J* values) were reported in Hertz (Hz). High resolution mass spectra were acquired using Bruker micrOTOF-Q instrument with an ESI ion source. The purity of the final compounds (>95%) was tested via HPLC on a Shimadzu LC-20A HPLC system installed with a UV detector. The HPLC methods was conducted using a 5 μm C-18 column (4.6 × 150 mm) at 40 ^{o}C and a flow rate of 1 mL/min. HPLC gradient, solvent A (water) and solvent B (methanol), 0-1 min 75 % B, 1-15 min 75-90 % B (linear gradient), 15-20 min 90% B. UV detection at 254 nm. Purities of the compounds were established by integrating the areas for all peaks detected and reported for each compound in the following section.

*4.1.1. General synthetic procedure for the key intermediate **3***

To a solution of 3,4,5-trimethoxyacetophenone (10 g, 47.6 mmol) in 40 mL DMF was added *N*, *N*-dimethylformamide dimethyl acetal (6.8 g, 57.1 mmol). The mixture was stirred at 120 ^{o}C for 6 h, then the reaction was quenched by H_2O, and extracted with CH_2Cl_2. concentrated in vacuo to provide the crude product, which was purified by column chromatography to give intermediate **2**. To a solution of **2** (2.4 g, 9.0 mmol) in 10 mL AcOH was added 3-bromo-1H-pyrazol-5-amine (1.5 g, 9.2 mmol). The mixture was stirred at 80 ^{o}C for 8h, after the reaction completed, the cooled mixture was deposited dropwise in H_2O, and the precipitate solid was filtered, dried to obtain intermediate **3**.

*4.1.2. General synthetic procedure for **1a-y***

To a solution of **3** (100 mg, 0.275 mmol) and corresponding boronic acid (0.360 mmol) in 5 mL DMF and 1 mL H_2O, Na_2CO_3 (73 mg, 0.688 mmol), $Pd(dppf)Cl_2$ (10 mg, 0.014 mmol) was added. The mixture was stirred at 95 ^{o}C for 12h, then the reaction was quenched by H_2O, and extracted with CH_2Cl_2. The combined organic layers were washed with brine, dried over anhydrous Na_2SO_4, and concentrated in vacuo to provide the crude product, which was purified by column chromatography with DCM/MeOH (100:1) to give pure compounds **1a-y**.

*4.1.3. General synthetic procedure for **4a-b***

The compounds **4a-b** were prepared from 4-fluoroacetophenone following the same procedure as described in preparation of compounds **1a-y**.

*4.1.4. General synthetic procedure for **1aa***

To a solution of **1y** (100 mg, 0.185 mmol) in 10 mL EtOH, 1mL H_2O was added NaOH (72 mg, 1.8 mmol). The mixture was stirred at 70 ^oC for 8h, then the reaction mixture was poured into water and extracted with CH_2Cl_2. The combined organic layers were washed with brine, dried over anhydrous Na_2SO_4, and concentrated in vacuo to provide the crude product. Which was purified by column chromatography with DCM/MeOH (90:1) to give the pure compound **1aa**.

*4.1.5. General synthetic procedure for **1ab**, **1ae***

To a solution of **1aa** (100 mg, 0.250 mmol) in 10 mL dry THF was added NaH (60 mg, 2.5 mmol). after stirring for 2h at 0 ^oC, then 0.6 mL CH_3I was added, the mixture was stirred at room temperature for 4h. the reaction was quenched by H_2O, and extracted with CH_2Cl_2. The combined organic layers were washed with brine, dried over anhydrous Na_2SO_4, and concentrated in vacuo to provide the crude product, which was purified by column chromatography with DCM/MeOH (85:1) to give pure compound **1ab**. The synthesis of compound **1ae** is similar to compound **1ab**.

*4.1.6. General synthetic procedure for **1ac***

To a solution of **1aa** (50 mg, 0.125 mmol) in 5 mL EtOH was added 1 mL 10% NaOH aqueous, 1 mL 37% HCHO aqueous. after stirring for 4h at room temperature. then the reaction mixture was poured into water and extracted with CH_2Cl_2. The combined organic layers were washed with brine, dried over anhydrous Na_2SO_4, and concentrated in vacuo to provide the crude product, which was purified by column chromatography with DCM/MeOH (80:1) to give pure compound **1ac**.

*4.1.7. General synthetic procedure for **1ad***

To a solution of **1q** (100 mg, 0.231 mmol) in 10 mL dry THF was added $LiAlH_4$ (87 mg, 2.3 mmol, the mixture was stirred at room temperature for 4h. The reaction was quenched by H_2O, and extracted with CH_2Cl_2. The combined organic layers were washed with brine, dried over anhydrous Na_2SO_4, and concentrated in vacuo to provide the crude product, which was purified by column chromatography with DCM/MeOH (85:1) to give pure compound **1ad**.

*4.1.8. General synthetic procedure for **1af***

To a solution of **1h** (50 mg, 0.115 mmol) in 2 mL THF, 3mL MeOH was added 10 mg 10% Pd/C. The reaction system was replaced by nitrogen three times, hydrogenated with H_2 at room temperature and monitored by TLC. The catalyst was filtered and the solvent was removed in vacuum to afford the compound **1af**.

*4.1.9. General synthetic procedure for **7***

To a solution of **2** (2.4 g, 9.0 mmol) in 10 mL AcOH was added 4-bromo-1H-pyrazol-5-amine (1.5 g, 9.2 mmol). The mixture was stirred at 80 ^oC for 8h, after the reaction completed, the cooled mixture was deposited dropwise in H_2O, and the precipitate solid was filtered, dried to obtain the intermediate **5**. Then compound **7** was synthesized according to the synthesis procedure of **1aa**.

*4.1.10. General synthetic procedure for **11***

To a solution of 3-acetylindole (5 g, 31.4 mmol) in 30 mL dry THF was added NaH, after 6 hours, benzenesulfonyl chloride (6.6 g, 37.7 mmol) was added. The mixture was

stirred at 25 ^{o}C for 6h, then the reaction was quenched by H_2O, and extracted with CH_2Cl_2, and concentrated in vacuo to provide the intermediate **8**. Then compound **11** was synthesized according to the synthesis procedure of **1n**.

4.1.11. 2-(1-methyl-1*H*-indol-5-yl)-7-(3,4,5-trimethoxyphenyl)pyrazolo[1,5-*a*]pyrimidine (**1a**). Yield: 81.5 %; mp 177-179 ^{o}C; ^{1}H NMR (400 MHz, $CDCl_3$) δ 8.43 (s, 1H), 8.31 (s, 1H), 7.94 (d, *J* = 8.5 Hz, 1H), 7.59 (s, 2H), 7.36 (d, *J* = 11.5 Hz, 1H), 7.11 (s, 1H), 7.06 (s, 1H), 6.85 (s, 1H), 6.56 (s, 1H), 4.01 (s, 3H), 3.99 (s, 3H), 3.77 (s, 3H). ^{13}C NMR (101 MHz, $CDCl_3$) δ 157.19, 153.00, 151.33, 148.53, 145.53, 140.37, 137.23, 129.63, 128.68, 126.15, 124.19, 120.32, 119.23, 109.43, 107.12, 106.22, 101.60, 92.92, 60.95, 56.32, 32.83. HRMS *m/z*: calcd for $C_{24}H_{22}N_4O_3$ $[M+H]^+$ 415.1765, found 415.1783. Purity: 98.1 % by HPLC (t_R = 7.93 min).

4.1.12. 2-(*p*-tolyl)-7-(3,4,5-trimethoxyphenyl)pyrazolo[1,5-*a*]pyrimidine (**1b**). Yield: 88.0 %; mp 155-157 ^{o}C; ^{1}H NMR (400 MHz, $CDCl_3$) δ 8.48 (d, *J* = 4.4 Hz, 1H), 7.92 (d, *J* = 8.1 Hz, 2H), 7.54 (s, 2H), 7.28 (d, *J* = 7.9 Hz, 2H), 7.06 (s, 1H), 6.91 (d, *J* = 4.4 Hz, 1H), 4.00 (s, 3H), 3.98 (s, 6H), 2.41 (s, 3H). ^{13}C NMR (101 MHz, $CDCl_3$) δ 155.83, 153.03, 151.17, 148.71, 145.85, 140.43, 138.97, 129.97, 129.42, 126.31, 125.92, 115.19, 107.04, 106.57, 93.24, 60.96, 56.32, 21.34. HRMS *m/z*: calcd for $C_{22}H_{21}N_3O_3$ $[M+H]^+$ 376.1656, found 376.1676. Purity: 98.5 % by HPLC (t_R = 9.56 min).

4.1.13. 2-(1*H*-indol-6-yl)-7-(3,4,5-trimethoxyphenyl)pyrazolo[1,5-*a*]pyrimidine (**1c**). Yield: 80.2 %; ^{1}H NMR (400 MHz, $CDCl_3$) δ 8.49 (d, *J* = 4.4 Hz, 1H), 8.40 (s, 1H), 8.09 (s, 1H), 7.84 (d, *J* = 8.2 Hz, 1H), 7.73 (d, *J* = 8.2 Hz, 1H), 7.56 (s, 2H), 7.13 (s, 1H), 6.91

(d, *J* = 4.4 Hz, 1H), 6.61 (s, 1H), 4.00 (s, 9H). ^{13}C NMR (101 MHz, $CDCl_3$) δ 156.98, 153.07, 151.30, 148.62, 145.80, 140.43, 136.06, 128.70, 126.79, 126.14, 125.46, 120.85, 118.74, 109.13, 107.10, 106.43, 102.79, 93.28, 60.96, 56.37. HRMS *m/z*: calcd for $C_{23}H_{20}N_4O_3$ $[M+H]^+$ 401.1609, found 401.1617. Purity: 97.8 % by HPLC (t_R = 5.32 min).

4.1.14. 7-(3,4,5-trimethoxyphenyl)-2-(4-vinylphenyl)pyrazolo[1,5-*a*]pyrimidine (**1d**). Yield: 79.8 %; ^{1}H NMR (400 MHz, $CDCl_3$) *δ* 8.48 (d, *J* = 4.4 Hz, 1H), 7.98 (d, *J* = 8.2 Hz, 2H), 7.57 – 7.47 (m, 4H), 7.07 (s, 1H), 6.91 (d, *J* = 4.4 Hz, 1H), 6.78 (dd, *J* = 18.6, 7.7 Hz, 1H), 5.82 (d, *J* = 17.6 Hz, 1H), 5.30 (d, *J* = 10.6 Hz, 1H), 3.99 (ss, 9H). ^{13}C NMR (100 MHz, $CDCl_3$) δ 155.28, 153.04, 151.25, 149.75, 148.83, 145.79, 140.50, 138.13, 136.32, 132.19, 126.52, 125.85, 114.34, 107.07, 106.73, 93.52, 60.94, 56.33. HRMS *m/z*: calcd for $C_{23}H_{21}N_3O_3$ $[M+H]^+$ 388.1656, found 388.1676. Purity: 97.2 % by HPLC (t_R = 10.72 min).

4.1.15. 2-(3,4-dimethylphenyl)-7-(3,4,5-trimethoxyphenyl)pyrazolo[1,5-*a*]pyrimidine (**1e**). Yield: 86.4 %; ^{1}H NMR (400 MHz, $CDCl_3$) *δ* 8.48 (d, *J* = 4.3 Hz, 1H), 7.83 (s, 1H), 7.76 (d, *J* = 7.8 Hz, 1H), 7.57 (s, 2H), 7.24 (d, *J* = 7.8 Hz, 1H), 7.05 (s, 1H), 6.92 (d, *J* = 4.3 Hz, 1H), 4.00 (ss, 9H), 2.36 (s, 3H), 2.33 (s, 3H). ^{13}C NMR (100 MHz, $CDCl_3$) δ 155.91, 153.04, 151.23, 148.68, 145.71, 140.45, 137.65, 136.84, 130.35, 129.99, 127.57, 125.96, 123.88, 107.07, 106.47, 93.24, 60.95, 56.29, 19.86, 19.65. HRMS *m/z*: calcd for $C_{23}H_{23}N_3O_3$ $[M+H]^+$ 390.1813, found 390.1829. Purity: 98.0 % by HPLC (t_R = 11.90 min).

4.1.16.N,N-dimethyl-4-(7-(3,4,5-trimethoxyphenyl)pyrazolo[1,5-*a*]pyrimidin-2-yl)aniline (**1f**). Yield: 88.3 %; ^{1}H NMR (400 MHz, $CDCl_3$) δ 8.43 (d, J = 4.3 Hz, 1H), 7.91 (d, J = 8.9 Hz, 2H), 7.56 (s, 2H), 6.96 (s, 1H), 6.85 (d, J = 4.4 Hz, 1H), 6.79 (d, J = 8.9 Hz, 2H), 3.99 (ss, 9H), 3.02 (s, 6H). ^{13}C NMR (101 MHz, $CDCl_3$) δ 156.35, 153.47, 152.98, 150.95, 148.42, 145.44, 140.35, 127.38, 126.17, 120.70, 112.13, 107.09, 106.01, 92.15, 60.93, 56.33, 40.29. HRMS *m/z*: calcd for $C_{23}H_{24}N_4O_3$ $[M+H]^+$ 405.1922, found 405.1941. Purity: 96.3 % by HPLC (t_R = 8.68 min).

4.1.17. 2-phenyl-7-(3,4,5-trimethoxyphenyl)pyrazolo[1,5-*a*]pyrimidine (**1g**). Yield: 80.0 %; ^{1}H NMR (400 MHz, $CDCl_3$) δ 8.49 (d, J = 4.4 Hz, 1H), 8.03 (d, J = 8.3 Hz, 2H), 7.53 (s, 2H), 7.47 (t, J = 7.4 Hz, 2H), 7.41 (d, J = 7.2 Hz, 1H), 7.09 (s, 1H), 6.92 (d, J = 4.4 Hz, 1H), 3.99 (s, 3H), 3.98 (s, 6H). ^{13}C NMR (101 MHz, $CDCl_3$) δ 155.68, 153.04, 151.23, 148.86, 145.88, 140.45, 132.80, 128.96, 128.71, 126.41, 125.88, 107.03, 106.75, 93.56, 60.96, 56.33. HRMS *m/z*: calcd for $C_{21}H_{19}N_3O_3$ $[M+H]^+$ 362.1500, found 362.1529. Purity: 97.2 % by HPLC (t_R = 7.43 min).

*4.1.18.*2-(4-methoxy-3-nitrophenyl)-7-(3,4,5-trimethoxyphenyl)pyrazolo[1,5-*a*]pyrimidin e (**1h**). Yield: 88.4 %; ^{1}H NMR (400 MHz, $CDCl_3$) δ 8.56 (d, J = 2.0 Hz, 1H), 8.52 (d, J = 4.4 Hz, 1H), 8.14 (dd, J = 2.0 Hz, J = 8.8 Hz, 1H), 7.53 (s, 2H), 7.19 (d, J = 8.8 Hz, 1H), 7.03 (s, 1H), 6.98 (d, J = 4.4 Hz, 1H), 4.03 (s, 3H), 4.00 (s, 9H). ^{13}C NMR (100 MHz, $CDCl_3$) δ 153.32, 153.11, 153.03, 151.42, 149.20, 145.87, 140.71, 139.66, 131.86, 125.74, 125.48, 123.66, 113.75, 107.08, 93.24, 60.97, 56.64, 56.36. ESI-MS *m/z*: $[M+H]^+$ 437. Purity: 96.3 % by HPLC (t_R = 6.00 min).

4.1.19.N,N-dimethyl-4-(7-(3,4,5-trimethoxyphenyl)pyrazolo[1,5-*a*]pyrimidin-2-yl)aniline (**1i**). Yield: 78.5 %; ^{1}H NMR (400 MHz, $CDCl_3$) δ 8.46 (s, 1H), 7.72 (t, *J* = 12.8 Hz, 2H), 7.49 (s, 2H), 7.02 (t, *J* = 8.4 Hz, 1H), 6.96 (s, 1H), 6.90 (s, 1H), 3.97 (s, 9H), 3.93 (s 3H). ^{13}C NMR (101 MHz, $CDCl_3$) δ 154.47, 153.65, 153.04, 151.30, 148.89, 148.32, 145.78, 140.53, 125.78, 122.39, 114.11, 113.92, 113.32, 107.04, 106.72, 93.08, 60.93, 56.31, 56.19. HRMS *m/z*: calcd for $C_{22}H_{20}FN_3O_4$ $[M+H]^+$ 410.1511, found 410.1521. Purity: 96.0 % by HPLC (t_R = 7.27 min).

4.1.20. 2-(4-methoxyphenyl)-7-(3,4,5-trimethoxyphenyl)pyrazolo[1,5-*a*]pyrimidine (**1j**). Yield: 83.8 %; ^{1}H NMR (400 MHz, DMSO-d_6) δ 8.57 (d, *J* = 3.8 Hz, 1H), 8.00 (d, *J* = 7.9 Hz, 2H), 7.68 (s, 2H), 7.33 (s, 1H), 7.24 (s, 1H), 7.06 (d, *J* = 8.4 Hz, 2H), 3.92 (s, 7H), 3.82 (d, *J* = 4.7 Hz, 7H). ^{13}C NMR (101 MHz, DMSO-d_6) δ 160.43, 154.96, 152.99, 151.32, 149.76, 145.06, 140.19, 127.92, 126.01, 125.42, 114.76, 107.70, 104.92, 92.89, 60.61, 56.56, 55.63. HRMS *m/z*: calcd for $C_{22}H_{21}N_3O_4$ $[M+H]^+$ 392.1605, found 392.1622. Purity: 95.8 % by HPLC (t_R = 7.18 min).

*4.1.21.*9-ethyl-3-(7-(3,4,5-trimethoxyphenyl)pyrazolo[1,5-*a*]pyrimidin-2-yl)-9H-carbazole (**1k**). Yield: 84.2 %; ^{1}H NMR (400 MHz, DMSO-d_6) δ 8.87 (s, 1H), 8.58 (s, 1H), 8.21 (d, *J* = 8.0 Hz, 2H), 7.78 (s, 2H), 7.72 (d, *J* = 8.5 Hz, 1H), 7.64 (d, *J* = 8.1 Hz, 1H), 7.49 (t, *J* = 7.4 Hz, 1H), 7.39 (s, 1H), 7.38 – 7.34 (m, 2H), 7.26 (t, *J* = 7.3 Hz, 1H), 4.48 (d, *J* = 6.7 Hz, 3H), 3.98 (s, 6H), 3.84 (s, 3H), 1.34 (t, *J* = 6.4 Hz, 5H). ^{13}C NMR (101 MHz, DMSO-d_6) δ 156.18, 153.03, 151.47, 149.68, 144.92, 140.46, 140.42, 140.23, 126.48, 126.06, 124.43, 123.78, 122.92, 122.66, 120.80, 119.56, 118.72, 109.88, 109.78, 107.76,

107.46, 92.95, 60.64, 56.54, 37.51, 14.13. HRMS *m/z*: calcd for $C_{29}H_{26}N_4O_3$ $[M+H]^+$ 479.2078, found 479. 2102. Purity: 96.8 % by HPLC (t_R = 16.00 min).

*4.1.22.*2-(1-methyl-1*H*-indazol-5-yl)-7-(3,4,5-trimethoxyphenyl)pyrazolo[1,5-*a*]pyrimidine (**1l**). Yield: 86.1 %; ^{1}H NMR (400 MHz, DMSO-d_6) δ 8.58 (d, J = 4.4 Hz, 1H), 8.46 (s, 1H), 8.13 - 8.16 (m, 2H), 7.77 - 7.70 (m, 3H), 7.37 - 7.34 (m, 2H), 4.08 (s, 3H), 3.94 (s, 6H), 3.82 (s, 3H). ^{13}C NMR (101 MHz, DMSO-d_6) δ 155.53, 153.63, 153.02, 151.35, 149.87, 145.13, 140.26, 133.59, 126.03, 125.47, 124.88, 124.26, 119.07, 110.58, 107.71, 104.96, 93.25, 60.63, 56.57, 35.87. HRMS *m/z*: calcd for $C_{23}H_{21}N_5O_3$ $[M+H]^+$ 416.1718, found 416.1720. Purity: 95.8 % by HPLC (t_R = 4.97 min).

4.1.23. 2-(*m*-tolyl)-7-(3,4,5-trimethoxyphenyl)pyrazolo[1,5-*a*]pyrimidine (**1m**). Yield: 80.9 %; ^{1}H NMR (400 MHz, $CDCl_3$) δ 8.47 (s, 1H), 7.89 - 7.75 (m, 2H), 7.54 (s, 2H), 7.35 (s, 1H), 7.22 (d, 1H), 7.07 (s, 1H), 6.91 (s, 1H), 3.98 (s, 9H), 2.43 (s, 3H). ^{13}C NMR (101 MHz, $CDCl_3$) δ 155.76, 153.49, 153.02, 148.74, 145.73, 140.48, 138.25, 132.69, 129.72, 128.61, 127.05, 125.87, 123.55, 107.08, 104.50, 93.50, 60.92, 56.28, 21.45. HRMS *m/z*: calcd for $C_{22}H_{21}N_3O_3$ $[M+H]^+$ 376.1606, found 376.1673. Purity: 95.6 % by HPLC (t_R = 9.76 min).

4.1.24. 2,7-bis(3,4,5-trimethoxyphenyl)pyrazolo[1,5-*a*]pyrimidine (**1n**). Yield: 85.5 %; ^{1}H NMR (400 MHz, $CDCl_3$) δ 8.51 (d, J = 4.3 Hz, 1H), 7.55 (s, 2H), 7.27 (s, 2H), 7.04 (s, 1H), 6.95 (d, J = 4.4 Hz, 1H), 3.99 (ss, 9H), 3.97 (s, 6H), 3.92 (s, 3H). ^{13}C NMR (101 MHz, $CDCl_3$) δ 155.56, 153.48, 153.05, 151.29, 148.91, 145.78, 140.55, 138.98, 128.42, 125.84, 107.10, 106.73, 103.66, 93.46, 60.99, 60.93, 56.27, 56.12. HRMS *m/z*: calcd for

$C_{24}H_{25}N_3O_6$ $[M+H]^+$ 452.1817, found 452.1831. Purity: 98.4 % by HPLC (t_R = 5.19 min).

*4.1.25.*4-(4-(7-(3,4,5-trimethoxyphenyl)pyrazolo[1,5-*a*]pyrimidin-2-yl)phenyl)morpholine (**1o**). Yield: 83.4 %; ^{1}H NMR (400 MHz, Chloroform-*d*) δ 8.46 (d, *J* = 4.3 Hz, 1H), 7.94 (d, *J* = 8.5 Hz, 2H), 7.53 (s, 2H), 6.98 (ss, 3H), 6.89 (d, *J* = 4.3 Hz, 1H), 3.98 (d, *J* = 2.9 Hz, 9H), 3.88 (t, *J* = 4.4 Hz, 4H), 3.24 (t, *J* = 4.4 Hz, 4H). ^{13}C NMR (101 MHz, $CDCl_3$) δ 155.78, 153.03, 151.68, 151.32, 148.61, 145.67, 140.44, 127.41, 126.04, 124.19, 115.20, 107.09, 106.31, 92.66, 66.75, 60.95, 56.34, 48.72. HRMS *m/z*: calcd for $C_{25}H_{26}N_4O_4$ $[M+H]^+$ 447.2027, found 447.2049. Purity: 96.2 % by HPLC (t_R = 5.70 min).

*4.1.26.*2-(1-methyl-1*H*-pyrazol-4-yl)-7-(3,4,5-trimethoxyphenyl)pyrazolo[1,5-*a*]pyrimidine (**1p**). Yield: 85.8 %; ^{1}H NMR (400 MHz, $CDCl_3$) δ 8.47 (s, 1H), 7.96 (s, 1H), 7.85 (s, 1H), 7.47 (s, 2H), 6.88 (s, 1H), 6.82 (s, 1H), 4.06 - 3.92 (m, 12H). ^{13}C NMR (101 MHz, $CDCl_3$) δ 153.07, 151.00, 149.76, 148.75, 145.73, 140.48, 137.80, 128.30, 125.95, 116.16, 107.04, 106.42, 93.11, 60.93, 56.33, 39.09. HRMS *m/z*: calcd for $C_{19}H_{19}N_5O_3$ $[M+H]^+$ 366.1561, found 366.1569. Purity: 97.8 % by HPLC (t_R = 2.79 min).

4.1.27. ethyl 4-(7-(3,4,5-trimethoxyphenyl)pyrazolo[1,5-*a*]pyrimidin-2-yl)benzoate (**1q**). Yield: 83.7 %; ^{1}H NMR (400 MHz, $CDCl_3$) δ 8.54 (d, *J* = 4.3 Hz, 1H), 8.15 (d, *J* = 8.5 Hz, 2H), 8.10 (d, *J* = 8.4 Hz, 2H), 7.53 (s, 2H), 7.16 (s, 1H), 6.98 (d, *J* = 4.3 Hz, 1H), 4.43 (q, *J* = 7.1 Hz, 2H), 4.00 (ss, 9H), 1.44 (t, *J* = 7.1 Hz, 3H). ^{13}C NMR (100 MHz, $CDCl_3$) δ 166.27, 154.51, 153.12, 151.18, 149.08, 146.12, 140.66, 136.98, 130.64, 129.98,

126.21, 125.63, 107.07, 94.30, 60.98, 56.36, 14.29. HRMS *m/z*: calcd for $C_{24}H_{23}N_3O_5$ $[M+H]^+$ 434.1711, found 434.1720. Purity: 98.0 % by HPLC (t_R = 9.77 min).

4.1.28.t-butyl-3-(7-(3,4,5-trimethoxyphenyl)pyrazolo[1,5-*a*]pyrimidin-2-yl)-1*H*-indole-1-carboxylate (**1r**). Yield: 80.6 %; ^{1}H NMR (400 MHz, $CDCl_3$) δ 8.52 (d, *J* = 4.4 Hz, 1H), 8.46 (d, *J* = 7.8 Hz, 1H), 8.24 (d, *J* = 8.0 Hz, 1H), 8.15 (s, 1H), 7.56 (s, 2H), 7.41 (t, *J* = 7.6 Hz, 1H), 7.33 (t, *J* = 7.6 Hz, 1H), 7.09 (s, 1H), 6.93 (d, *J* = 4.4 Hz, 1H), 4.02 (ss, 9H), 1.74 (s, 8H). ^{13}C NMR (100 MHz, $CDCl_3$) δ 153.12, 151.01, 150.66, 149.48, 149.02, 145.90, 140.53, 135.80, 128.13, 126.16, 124.84, 123.08, 121.84, 115.23, 114.31, 107.03, 106.52, 93.82, 84.23, 61.00, 56.33, 28.16. HRMS *m/z*: calcd for $C_{28}H_{28}N_4O_5$ $[M+H]^+$ 501.2133, found 501.2142. Purity: 98.8 % by HPLC (t_R = 17.82 min).

4.1.29. 2-(4-fluorophenyl)-7-(3,4,5-trimethoxyphenyl)pyrazolo[1,5-*a*]pyrimidine (**1s**). Yield: 85.0 %; ^{1}H NMR (400 MHz, $CDCl_3$) δ 8.49 (d, *J* = 4.1 Hz, 1H), 7.99 (t, *J* = 6.0 Hz, 2H), 7.50 (s, 2H), 7.15 (t, *J* = 8.4 Hz, 2H), 7.03 (s, 1H), 6.93 (d, *J* = 3.9 Hz, 1H), 3.98 (ss, 9H). ^{13}C NMR (101 MHz, $CDCl_3$) δ 154.81, 153.09, 151.29, 148.95, 145.98, 140.57, 132.07, 128.12, 125.81, 115.81, 115.59, 107.07, 106.83, 93.35, 60.95, 56.35. HRMS *m/z*: calcd for $C_{21}H_{18}FN_3O_3$ $[M+H]^+$ 380.1405, found 380.1430. Purity: 96.5 % by HPLC (t_R = 7.72 min).

4.1.30. 3-(7-(3,4,5-trimethoxyphenyl)pyrazolo[1,5-*a*]pyrimidin-2-yl)benzonitrile (**1t**). Yield: 82.3 %; ^{1}H NMR (400 MHz, $CDCl_3$) δ 8.56 (d, *J* = 4.4 Hz, 1H), 8.33 (s, 1H), 8.24 (d, *J* = 7.9 Hz, 1H), 7.69 (d, *J* = 7.7 Hz, 1H), 7.60 (d, *J* = 7.8 Hz, 1H), 7.48 (s, 2H), 7.12 (s, 1H), 7.00 (d, *J* = 4.4 Hz, 1H), 4.01 (ss, 9H). ^{13}C NMR (101 MHz, $CDCl_3$) δ 153.26,

153.16, 151.29, 149.37, 146.23, 140.74, 134.23, 132.08, 130.49, 129.92, 129.58, 125.50, 118.55, 112.98, 107.46, 107.04, 93.94, 60.99, 56.37. ESI-MS *m/z*: $[M+H]^+$ 387. Purity: 96.0 % by HPLC (t_R = 5.33 min).

4.1.31.1-(4-(7-(3,4,5-trimethoxyphenyl)pyrazolo[1,5-*a*]pyrimidin-2-yl)phenyl)ethan-1-one (**1u**). Yield: 81.9 %; ^{1}H NMR (400 MHz, Chloroform-*d*) δ 8.55 (d, *J* = 4.4 Hz, 1H), 8.14 (d, *J* = 8.4 Hz, 2H), 8.07 (d, *J* = 8.4 Hz, 2H), 7.52 (s, 2H), 7.17 (s, 1H), 6.99 (d, *J* = 4.4 Hz, 1H), 4.01 (d, *J* = 3.6 Hz, 9H), 2.67 (s, 3H). ^{13}C NMR (101 MHz, $CDCl_3$) δ 197.53, 154.23, 153.09, 151.25, 149.15, 146.01, 140.66, 137.23, 137.07, 128.78, 126.39, 125.61, 107.22, 107.09, 94.37, 60.96, 56.35, 26.60. ESI-MS *m/z*: $[M+H]^+$ 404. Purity: 96.4 % by HPLC (t_R = 5.05 min).

4.1.32.2-(4-(trifluoromethyl)phenyl)-7-(3,4,5-trimethoxyphenyl)pyrazolo[1,5-*a*]pyrimidine (**1v**). Yield: 83.1 %; ^{1}H NMR (400 MHz, $CDCl_3$) δ 8.56 (s, 1H), 8.15 (d, *J* = 6.4 Hz, 2H), 7.75 (t, *J* = 8.0 Hz, 2H), 7.51 (s, 2H), 7.15 (s, 1H), 6.99 (s, 1H), 4.01 (ss, 9H). ^{13}C NMR (101 MHz, $CDCl_3$) δ 153.53, 153.08, 151.25, 149.16, 145.98, 140.66, 136.27, 134.60, 132.27, 126.52, 125.59, 107.21, 107.06, 104.55, 94.13, 60.93, 56.30. ESI-MS *m/z*: $[M+H]^+$ 430. Purity: 96.1 % by HPLC (t_R = 11.14 min).

4.1.33. 2-(4-chlorophenyl)-7-(3,4,5-trimethoxyphenyl)pyrazolo[1,5-*a*]pyrimidine (**1w**). Yield: 84.4 %; ^{1}H NMR (400 MHz, $CDCl_3$) δ 8.53 (s, 1H), 7.97 (d, *J* = 6.7 Hz, 2H), 7.50 (s, 2H), 7.45 (d, *J* = 8.1 Hz, 2H), 7.07 (s, 1H), 6.96 (s, 1H), 4.02 (ss, 9H). ^{13}C NMR (101 MHz, $CDCl_3$) δ 154.47, 153.06, 151.25, 148.98, 145.90, 140.57, 134.77, 131.33, 128.88, 127.59, 125.72, 107.05, 104.54, 93.54, 60.94, 56.33. ESI-MS *m/z*: $[M+H]^+$ 396. Purity:

96.4 % by HPLC (t_R = 10.67 min).

4.1.34. 2-(4-(*t*-butyl)phenyl)-7-(3,4,5-trimethoxyphenyl)pyrazolo[1,5-*a*]pyrimidine (**1x**). Yield: 83.7 %; ^{1}H NMR (400 MHz, $CDCl_3$) δ 8.48 (d, *J* = 4.3 Hz, 1H), 7.97 (d, *J* = 8.3 Hz, 2H), 7.55 (s, 2H), 7.50 (d, *J* = 8.5 Hz, 2H), 7.07 (s, 1H), 6.92 (d, *J* = 4.4 Hz, 1H), 3.99 (ss, 9H), 1.38 (s, 9H). ^{13}C NMR (101 MHz, $CDCl_3$) δ 153.51, 153.02, 151.24, 148.69, 145.77, 140.47, 134.60, 130.03, 126.16, 125.65, 107.11, 106.52, 104.53, 93.33, 60.95, 56.35, 34.69, 31.22. ESI-MS *m/z*: $[M+H]^+$ 418. Purity: 95.3 % by HPLC (t_R = 15.35 min).

4.1.35. 2-(1*H*-indol-3-yl)-7-(3,4,5-trimethoxyphenyl)pyrazolo[1,5-*a*]pyrimidine (**1aa**). Yield: 74.3%; ^{1}H NMR (400 MHz, $CDCl_3$) δ 8.83 (s, 1H), 8.46 - 8.48 (m, 2H), 7.74 (s, 1H), 7.59 (s, 2H), 7.41 (d, *J* = 7.5 Hz, 1H), 7.28 (m, 1H), 7.02 (s, 1H), 6.89 (d, *J* = 3.9 Hz, 1H), 4.01 (ss, 9H). ^{13}C NMR (101 MHz, $CDCl_3$) δ 153.08, 152.81, 150.74, 148.61, 145.77, 140.42, 136.53, 126.44, 125.35, 124.19, 122.67, 121.49, 120.62, 111.37, 110.32, 107.10, 106.03, 92.72, 61.00, 56.35. HRMS *m/z*: calcd for $C_{23}H_{20}N_4O_3$ $[M+H]^+$ 401.1609, found 401.1620. Purity: 98.6 % by HPLC (t_R = 4.80 min).

4.1.36. 2-(1-methyl-1*H*-indol-3-yl)-7-(3,4,5-trimethoxyphenyl)pyrazolo[1,5-*a*]pyrimidine (**1ab**). Yield: 72.5%; ^{1}H NMR (400 MHz, $CDCl_3$) δ 8.51 - 8.41 (m, 2H), 7.66 (s, 1H), 7.59 (s, 2H), 7.40 (d, *J* = 8.2 Hz, 1H), 7.33 (t, *J* = 7.2 Hz, 1H), 7.24 (t, *J* = 7.1 Hz, 1H), 7.00 (s, 1H), 6.88 (d, *J* = 4.4 Hz, 1H), 4.02 (ss, 9H), 3.90 (s, 3H). ^{13}C NMR (101 MHz, $CDCl_3$) δ 153.07, 152.73, 150.81, 148.56, 145.66, 140.41, 137.38, 128.55, 126.49, 125.92, 122.30, 121.71, 120.34, 109.45, 108.88, 107.09, 105.90, 92.49, 60.99, 56.35, 33.06.

HRMS *m/z*: calcd for $C_{24}H_{22}N_4O_3$ $[M+H]^+$ 415.1765, found 415.1777. Purity: 98.7 % by HPLC (t_R = 7.70 min).

4.1.37.(3-(7-(3,4,5-trimethoxyphenyl)pyrazolo[1,5-*a*]pyrimidin-2-yl)-1*H*-indol-1-yl)methanol (**1ac**). Yield: 67.0%; ^{1}H NMR (400 MHz, $CDCl_3$) δ 8.35 (dd, *J* = 4.4 Hz, *J* = 8.0 Hz, 2H), 7.72 (s, 1H), 7.49 (m, 3H), 7.46, 7.23 (tt, *J* = 8.0 Hz, *J* = 8.0 Hz, 2H), 6.90 (s, 1H), 6.82 (d, *J* = 4.4 Hz, 1H), 5.55 (s, 2H), 3.90 (s, 9H). ^{13}C NMR (100 MHz, $CDCl_3$) δ 156.93, 156.89, 154.11, 152.52, 150.13, 144.20, 140.41, 131.56, 130.33, 130.26, 126.44, 125.34, 124.59, 113.90, 113.41, 111.02, 110.04, 96.06, 73.07, 64.55, 59.96. HRMS *m/z*: calcd for $C_{24}H_{22}N_4O_4$ $[M+H]^+$ 431.1714, found 431.1719. Purity: 98.0 % by HPLC (t_R = 3.96 min).

4.1.38. (4-(7-(3,4,5-trimethoxyphenyl)pyrazolo[1,5-*a*]pyrimidin-2-yl)phenyl)methanol (**1ad**). Yield: 86.4%; ^{1}H NMR (400 MHz, $CDCl_3$) δ 8.41 (d, *J* = 4.4 Hz, 1H), 7.94 (d, *J* = 8.0 Hz, 2H), 7.46 (s, 2H), 7.41 (d, *J* = 8.0 Hz, 2H), 7.00 (s, 1H), 6.90 (d, *J* = 4.4 Hz, 1H), 4.66 (s, 2H), 3.92 (s, 9H). ^{13}C NMR (101 MHz, $CDCl_3$) δ 155.62, 152.95, 150.87, 148.72, 146.10, 142.08, 140.43, 131.68, 127.14, 126.42, 125.73, 107.04, 106.70, 93.30, 64.26, 60.87, 56.24. HRMS *m/z*: calcd for $C_{22}H_{21}N_3O_4$ $[M+H]^+$ 392.1605, found 392.1608. Purity: 98.3 % by HPLC (t_R = 3.23 min).

4.1.39. 2-(1-methyl-1*H*-indol-6-yl)-7-(3,4,5-trimethoxyphenyl)pyrazolo[1,5-*a*]pyrimidine (**1ae**). Yield: 77.3%; ^{1}H NMR (400 MHz, $CDCl_3$) δ 8.50 (d, *J* = 4.3 Hz, 1H), 8.04 (s, 1H), 7.82 (d, *J* = 8.2 Hz, 1H), 7.71 (d, *J* = 8.2 Hz, 1H), 7.62 (s, 2H), 7.15 (s, 1H), 7.13 (d, *J* = 3.0 Hz, 1H), 6.93 (d, *J* = 3.9 Hz, 1H), 6.53 (d, *J* = 2.8 Hz, 1H), 4.02 (ss, 9H), 3.88 (s, 3H).

^{13}C NMR (101 MHz, $CDCl_3$) δ 157.09, 153.06, 151.38, 148.61, 145.63, 140.45, 136.94, 130.13, 129.31, 126.30, 126.09, 120.99, 118.31, 107.19, 107.13, 106.33, 101.12, 93.30, 60.97, 56.31, 32.89. HRMS *m/z*: calcd for $C_{24}H_{22}N_4O_3$ $[M+H]^+$ 415.1765, found 415.1779. Purity: 97.3 % by HPLC (t_R = 8.27 min).

4.1.40. 2-methoxy-5-(7-(3,4,5-trimethoxyphenyl)pyrazolo[1,5-*a*]pyrimidin-2-yl)aniline (**1af**). Yield: 90.2%; ^{1}H NMR (400 MHz, $CDCl_3$) *δ* 8.48 (d, *J* = 4.4 Hz, 1H), 7.52 (s, 2H), 7.43 (m, 2H), 6.99 (s, 1H), 6.88 (m, 2H), 3.99 (ss 9H), 3.92 (s, 3H). ^{13}C NMR (100 MHz, $CDCl_3$) δ 156.04, 153.05, 151.21, 148.58, 148.22, 145.76, 140.44, 136.24, 126.08, 125.75, 117.09, 112.89, 110.37, 107.07, 106.37, 92.96, 60.94, 56.35, 55.52. ESI-MS *m/z*: $[M+H]^+$ 407. Purity: 98.9 % by HPLC (t_R = 3.61 min).

4.1.41. 7-(4-fluorophenyl)-2-(1-methyl-1H-indol-5-yl)pyrazolo[1,5-*a*]pyrimidine (**4a**). Yield: 73.5 %; ^{1}H NMR (400 MHz, $CDCl_3$) *δ* 8.44 (d, J = 4.3 Hz, 1H), 8.32 (s, 1H), 8.29 – 8.22 (m, 2H), 7.94 (d, J = 8.5 Hz, 1H), 7.39 (d, J = 8.6 Hz, 1H), 7.29 (t, J = 8.6 Hz, 2H), 7.13 (s, 1H), 7.09 (d, J = 3.0 Hz, 1H), 6.79 (d, J = 4.3 Hz, 1H), 6.60 (d, J = 2.9 Hz, 1H), 3.81 (s, 3H). ^{13}C NMR (101 MHz, CDCl3) δ 165.36, 162.85, 157.37, 151.17, 148.51, 144.93, 137.29, 131.72, 131.64, 129.59, 128.70, 124.12, 120.54, 119.33, 115.73, 115.51, 109.38, 106.34, 101.66, 93.13, 32.87. ESI-MS *m/z*: $[M+H]^+$ 343. Purity: 96.3 % by HPLC (t_R = 10.11 min).

4.1.42. 7-(4-fluorophenyl)-2-(*p*-tolyl)pyrazolo[1,5-*a*]pyrimidine (**4b**). Yield: 78.3 %; ^{1}H NMR (400 MHz, $CDCl_3$) *δ* 8.48 (d, *J* = 4.4 Hz, 1H), 8.30 - 8.17 (m, 2H), 7.92 (d, *J* = 8.1 Hz, 2H), 7.34 - 7.22 (m, 4H), 7.06 (s, 1H), 6.85 (d, *J* = 4.4 Hz, 1H), 2.43 (s, 3H). ^{13}C

NMR (101 MHz, $CDCl_3$) δ 156.01, 151.02, 148.68, 145.17, 139.00, 131.69, 131.61, 129.39, 126.47, 115.77, 115.56, 115.19, 106.67, 93.39, 21.33. ESI-MS *m/z*: $[M+H]^+$ 304. Purity: 97.8 % by HPLC (t_R = 12.17 min).

4.1.43. 3-(1*H*-indol-3-yl)-7-(3,4,5-trimethoxyphenyl)pyrazolo[1,5-*a*]pyrimidine (**7**). Yield: 71.2%; ^{1}H NMR (400 MHz, $CDCl_3$) *δ* 8.66 (s, 1H), 8.58 (d, *J* = 4.1 Hz, 1H), 8.52 (s, 1H), 8.02 (d, *J* = 7.5 Hz, 1H), 7.96 (s, 1H), 7.47 (d, *J* = 7.7 Hz, 1H), 7.37 (s, 2H), 7.28-7.24 (m, 2H), 6.93 (d, *J* = 4.1 Hz, 1H), 3.98 (s, 9H). ^{13}C NMR (101 MHz, $CDCl_3$) δ 153.27, 148.06, 146.53, 145.90, 142.39, 140.32, 136.20, 126.21, 126.14, 122.54, 122.23, 120.07, 119.86, 111.35, 107.28, 107.24, 106.69, 106.17, 60.93, 56.34. HRMS *m/z*: calcd for $C_{23}H_{20}N_4O_3$ $[M+H]^+$ 401.1614, found 401.1622. Purity: 98.1 % by HPLC (t_R = 4.49 min).

4.1.44. 7-(1*H*-indol-3-yl)-2-(3,4,5-trimethoxyphenyl)pyrazolo[1,5-*a*]pyrimidine (**11**). Yield: 70.2 %; ^{1}H NMR (400 MHz, DMSO-d_6) *δ* 12.26 (s, 1H), 9.29 (d, *J* = 3.0 Hz, 1H), 8.54 (d, *J* = 4.7 Hz, 1H), 8.20 (d, *J* = 8.6 Hz, 1H), 7.64 (dd, *J* = 6.6, 2.0 Hz, 1H), 7.59 (d, *J* = 4.8 Hz, 1H), 7.46 (s, 2H), 7.36 - 7.28 (m, 3H), 3.94 (s, 6H), 3.74 (s, 3H). ^{13}C NMR (101 MHz, DMSO-d_6) δ 154.61, 153.68, 151.24, 149.35, 141.54, 138.68, 136.96, 133.64, 128.82, 125.40, 123.08, 121.71, 120.70, 113.18, 104.97, 104.70, 104.15, 93.37, 60.55, 56.40. HRMS *m/z*: calcd for $C_{23}H_{20}N_4O_3$ $[M+H]^+$ 401.1614, found 401.1635. Purity: 98.6 % by HPLC (t_R = 6.68 min).

4.2. Cell culture and cytotoxicity assay

The antiproliferative activities of final compounds were evaluated against a panel of

cell lines including: human breast cancer cell (MCF-7), human lung cancer cell (A549), human colon cancer cell (HCT-116), human cervical cancer cell (Hela) and murine melanoma cell (B16-F10) by using the CKK-8 assay, with PTX and colchicine as the positive control. Cells were cultured in RPMI-1640 medium containing 10% fetal bovine serum, incubated at 37 ^{o}C in a humidified 5% CO_2 incubator. Cells were seeded into 96-well plates at a density of 1-3 × 10^4 cells/well, treated with vehicle control (0.1% DMSO), PTX, colchicine, or test compounds (0.00098, 0.0039, 0.016, 0.0625, 0.25, 1.0, 4.0, 16, 64 μM), and incubated at 37 ^{o}C for 48 h. Then CCK8 was added and incubated for another 4 h. The optical density was detected with a microplate reader at 450 nm. The IC_{50} values were calculated in accordance with the dose-dependent curves, which were presented as mean ± standard deviation. All the experiments were repeated three times for each cell line.

4.3. Tubulin polymerization assay

Pig brain tubulin protein (>97 % pure) was isolated by three cycles of temperature-dependent assembly/disassembly in PEM buffer (pH 6.5, 100 mM PIPES, 2 mM EGTA and 1 mM $MgSO_4$) containing 1 mM GTP and 1 mM 2-mercaptoethanol. In the first cycle of polymerization, phenylmethylsulfonyl fluoride and glycerol were added to 0.2 mM and 4 M, respectively. Homogeneous tubulin was prepared from microtubule protein by phosphocellulose chromatography. The purified proteins were stored in aliquots at -70 ^{o}C. tubulin protein was mixed with different concentrations of test compounds in PEM buffer (100 mM PIPES, 1 mM EGTA and 1 mM $MgCl_2$) containing

1 mM GTP and 5 % glycerol. Microtubule polymerization was monitored at 37 °C by light scattering at 340 nm using a SPECTRA MAX 190 (Molecular Device) spectrophotometer.

4.4. Cell cycle analysis

MCF-7 cells were seeded into 6-well plates and incubated at 37 ^{o}C in a humidified 5% CO_2 incubator for 24 h, and then treated with or without compounds (**1a** and **1b)** at indicated concentrations for another 48 h. The collected cells were fixed by adding 70 % ethanol at 4 ^{o}C for 12 h. After the removal of ethanol, cells were resuspended in PBS containing 100 mL RNase A and 400 mL of propidium iodide for 30 min. The DNA content of the cells was measured using a FACS Calibur flow cytometer (Bectone Dickinson, San Jose, CA, USA).

4.5. Wound healing assays

MCF-7 cancer cells were grown in six-well plates for 24 h. Scratches were made in confluent monolayers by 200 μL pipette tips. Then, wounds were washed 2-3 times with PBS to remove non-adherent cell debris. The media containing different concentrations (0, 10, 20. 40 nM) of compound **1b** was added to Petri dishes. Cells migrated across the wound area were photographed using phase contrast microscopy at 0 and 24 h. The migration distance of cells in the wound area was measured manually.

4.6. Immunofluorescent Staining

B16-F10 melanoma cells were seeded into 24-well plates and then treated with vehicle control (0.1% DMSO), PTX, Colchicine and compound **1b**. Cells were washed

with PBS for three times, then fixed with 4% paraformaldehyde, permeabilized with 0.5% Triton X-100 for 15 min, and blocked for 20 min by adding 50-100 μL goat serum albumin. Cells were incubated with anti-tubulin antibody at 4 ^{o}C for 2 h, washed three times by PBS, and followed by staining with the fluorescence secondary antibody (Alexa Fluor 647 goat anti-rat lgG) and labeling of nuclei by 4,5-diamidino-2-phenylindole (DAPI). Cells were finally visualized by confocal microscope.

4.7. Liver microsomal stability assay

Liver microsomal stability study was conducted by Medicilon Preclinical Research LLC (Shanghai, China). Briefly, 0.5 μM of test compound **1b** was incubated in a total reaction volume of 0.75 mg/mL microsomal protein in buffer (6 mM NADPH in 0.1 M K-phosphate buffer, pH 7.4) at 37 ^{o}C in a shaking water bath. The total DMSO concentration in the reaction was less than 0.5 %. 15 μL of NADPH stock solution (6 mM) was added to the plates to start the reaction, sampling at 0.25 h, 0.5 h, 1 h, 2 h, and 4 h, by adding 135 μL of acetonitrile containing IS (internal standard) to the wells of corresponding plates, respectively, to stop the reaction. After quenching, shake the plates for 5 min (600 rpm/min) and then the sample would be stored at -80 ^{o}C until LC/MS analysis. Before LC/MS analysis, centrifuge the sample at 4000 rpm for 15 min. Transfer 80 μL of the supernatant from each well into a 96-well sample plate containing 80 μL of ultra-pure water for LC/MS analysis.

4.8. Protein expression and purification

The stathmin-like domain of RB3 (RB3-SLD) was transformed into and

overexpressed in Escherichia coli (E. coli) system. Cells were harvested and resuspended in the lysis buffer containing 20 mM Tris-HCl pH 8.0, 2 mM DTT, 1 mM EGTA with the antiprotease cocktail. Then the protein was purified via anion-exchange chromatography and gel filtration chromatography. The peak fractions from gel filtration column were concentrated (to 10 mg/mL) and stored at -80 ^{o}C until use. TTL protein was expressed and purified from E. coli as described before [34-36]. Briefly, the cells were induced overnight by adding IPTG at 25 ^{o}C in the LB medium. Then cells were harvested and sonicated in the lysis buffer. The soluble fraction of the lysate was loaded onto Ni-NTA affinity chromatography followed by gel filtration chromatography. The final pure sample was concentrated to 20 mg/mL and stored under -80 ^{o}C. The purity of RB3 and TTL were examined by SDS-PAGE. Porcine brain tubulin was supplied at 10 mg/mL in G-PEM (General tubulin buffer: 80 mM PIPES pH 6.9, 2 mM $MgCl_2$, 0.5 mM EGTA and 1 mM GTP) as a frozen liquid and saved at -80 ^{o}C until use.

4.9. Crystallization and crystal soaking

Detailed process to obtain crystals of T2R-TTL was described before [37, 38]. The protein complex containing RB3 (6 mg/mL), tubulin (10 mg/mL), and TTL (20 mg/mL) at the molar ratio of 2:1.3:1.2 (Tubulin: RB3: TTL), were incubated on ice supplemented with 10 mM DTT, 5 mM tyrosinol, and 1 mM AMPPCP, then the solution was concentrated to 20 mg/mL at 4 ^{o}C. The crystals were grown at 20 ^{o}C using the sitting-drop vapor diffusion method by adding 1.0 μL protein complex to 1.0 μL crystallization buffer containing 6% PEG, 5% glycerol, 0.1M MES, 30 mM $CaCl_2$, 30

mM $MgCl_2$, pH 6.7. The high-quality single crystal was obtained by Seeding method. Initial crystals could be observed after two days and then the crystal reached to the final size of around 200-300 μm in length within 3-5 days. For the compounds soaking to the crystals, compounds **1a** and **1b** were dissolved in DMSO at 10 mM concentration. The crystals were soaked with **1a** or **1b** (0.1 μL) at 20 ^{o}C for 12 h, respectively. The crystals were dumped quickly into the cryoprotectant (5% glycerol, 6% PEG, 30 mM $MgCl_2$, 30 mM $CaCl_2$, 0.1M MES, pH 6.7, contained 20％glycerol) and flash frozen in a 100 K liquid nitrogen for data collection.

4.10. X-Ray data collection and structure determination

The crystals of the T2R-TTL-compound complexes were mounted in nylon loops, and flash frozen in a cold nitrogen stream at 100K. The diffraction data were obtained on beam-lines BL19U1 at Shanghai Synchrotron Radiation Facility. The dataset was processed by the HKL3000 program package[39]. The model was manually built with Coot. All refinements were carried out with phenix refine module of Phenix program[40]. The quality of the model was checked by the PROCHECK program, and was shown to have a good stereochemistry based on the Ramachandran plot.

4.11. In vivo antitumor efficacy study

The animal protocols were approved by the National Institutional Animal Care and ethical Committee of Southern Medical University. Male C57/BL mice (4-6 weeks old) were purchased from SPF Biotechnology Co., Ltd (Beijing). 2×10^5 B16-F10 cells were injected into the right flank of each mouse. All mice were weighted and randomized into

4 groups (vehicle, **1b** at 10mg/kg, **1b** at 20mg/kg, and PTX at 10mg/kg). Compound **1b** and PTX were formulated in 5 % DMSO, 40 % PEG-300 and 55 % saline. 200 μL of **1b** or vehicle solution were administered to mice via intraperitoneally injection per day. Tumor volume was measured with a traceable electronic digital caliper every other day, and calculated by the formula of Volume = $\pi/6 \times L \times W^2$, where L is the length, and W is the width of a tumor. Mice were sacrificed when tumor size reached approximately 4000 mm^3. Tumors and major organs were excised, weighed, and preserved in 10% neutral formalin buffer for subsequent pathological examination.

Associated content

Supporting Information

^{1}H NMR, ^{13}C NMR, HRMS and HPLC spectra.

PDB ID Codes: 6LSN (**1a**) and 6LSM (**1b**), Authors will release the atomic coordinates and experimental data upon article publication.

Author Information

Corresponding Authors

*E-mail: jchen21@smu.edu.cn (J. Chen)

ORCID

Jianjun Chen: 0000-0001-5668-6572

Gang Li: 0000-0003-4191-7643

Notes

The authors declare no competing financial interest.

Acknowledgement

This work was supported by scientific research project of high level talents (No. C1051008) in Southern Medical University of China; Thousand Youth Talents Program (No. C1080092) from the Organization Department of the CPC Central Committee, China; International Science and Technology Cooperation Projects of Guangdong Province (No. G819310411); and Guangdong Basic and Applied Basic Research Foundation (No. 2019A1515110616). The authors thank Dr. Benoît Gigant (Institute for Integrative Biology of the Cell (I2BC), CEA, CNRS, Univ. Paris-Sud, Universite′ ParisSaclay, France) and Dr. Michel O. Steinmetz (Paul Scherrer Institute, Switzerland) for kindly providing the plasmids of RB3-SLD and TTL. Lingling Ma (Sichuan University) and Jiahong Lei (Sichuan University) for helping the crystal preparation. The X-ray work was partially supported by National Natural Science Foundation of China (No. 81703553), China Postdoctoral Science Foundation (No.2017M610607), and Sichuan Science and Technology Program Projects (2019YFS0003).

References

[1] J. Howard, A.A. Hyman, Dynamics and mechanics of the microtubule plus end, Nature, 422 (2003) 753-758.

[2] M.A. Jordan, L. Wilson, Microtubules as a target for anticancer drugs, Nat Rev Cancer, 4 (2004) 253-265.

[3] Y. Zhang, H. Yang, J. Liu, Q. Deng, P. He, Y. Lin, J. Jiang, X. Gu, M. Mo, H. Pan, X. Xiong, Y. Qiu, J. He, High expression levels of class III β-tubulin in resected non-small cell lung cancer patients are predictive of improved patient survival after

vinorelbine-based adjuvant chemotherapy, Oncol Lett, 6 (2013) 220-226.

[4] M.O. Steinmetz, A.E. Prota, Microtubule-Targeting Agents: Strategies To Hijack the Cytoskeleton, Trends in Cell Biology, 28 (2018) 776-792.

[5] J.J. Field, A. Kanakkanthara, J.H. Miller, Microtubule-targeting agents are clinically successful due to both mitotic and interphase impairment of microtubule function, Bioorgan Med Chem, 22 (2014) 5050-5059.

[6] Y.M. Liu, H.L. Chen, H.Y. Lee, J.P. Liou, Tubulin inhibitors: a patent review, Expert Opin Ther Pat, 24 (2014) 69-88.

[7] L. Fang, M. Zhang, L. Chen, H. Xiong, Y. Ge, W. Lu, X. Wu, B. Heng, D. Yu, S. Wu, Downregulation of nucleolar and spindle-associated protein 1 expression suppresses cell migration, proliferation and invasion in renal cell carcinoma, Oncol Rep, 36 (2016) 1506-1516.

[8] E. Porcu, R. Bortolozzi, G. Basso, G. Viola, Recent advances in vascular disrupting agents in cancer therapy, Future Med Chem, 6 (2014) 1485-1498.

[9] K. Mao, F. Liu, X. Liu, F.R. Khuri, A.I. Marcus, M. Li, W. Zhou, Re-expression of LKB1 in LKB1-mutant EKVX cells leads to resistance to paclitaxel through the up-regulation of MDR1 expression, Lung Cancer, 88 (2015) 131-138.

[10] Z. Yuan, H. Wang, Z. Hu, Y. Huang, F. Yao, S. Sun, B. Wu, Quercetin inhibits proliferation and drug resistance in KB/VCR oral cancer cells and enhances its sensitivity to vincristine, Nutr Cancer, 67 (2015) 126-136.

[11] L. Li, S.B. Jiang, X.X. Li, Y. Liu, J. Su, J.J. Chen, Recent advances in trimethoxyphenyl (TMP) based tubulin inhibitors targeting the colchicine binding site, European journal of medicinal chemistry, 151 (2018) 482-494.

[12] W. Li, H. Sun, S. Xu, Z. Zhu, J. Xu, Tubulin inhibitors targeting the colchicine binding site: a perspective of privileged structures, Future Med Chem, 9 (2017) 1765-1794.

[13] Y. Lu, J.J. Chen, M. Xiao, W. Li, D.D. Miller, An Overview of Tubulin Inhibitors

That Interact with the Colchicine Binding Site, Pharmaceutical research, 29 (2012) 2943-2971.

[14] Y. Lu, C.M. Li, Z. Wang, C.R. Ross, J. Chen, J.T. Dalton, W. Li, D.D. Miller, Discovery of 4-Substituted Methoxybenzoyl-aryl-thiazole as Novel Anticancer Agents: Synthesis, Biological Evaluation, and Structure-Activity Relationships, Journal of medicinal chemistry, 52 (2009) 1701-1711.

[15] J. Chen, Z. Wang, C.M. Li, Y. Lu, P.K. Vaddady, B. Meibohm, J.T. Dalton, D.D. Miller, W. Li, Discovery of novel 2-aryl-4-benzoyl-imidazoles targeting the colchicines binding site in tubulin as potential anticancer agents, Journal of medicinal chemistry, 53 (2010) 7414-7427.

[16] J. Chen, S. Ahn, J. Wang, Y. Lu, J.T. Dalton, D.D. Miller, W. Li, Discovery of Novel 2-Aryl-4-benzoyl-imidazole (ABI-III) Analogues Targeting Tubulin Polymerization As Antiproliferative Agents, Journal of medicinal chemistry, 55 (2012) 7285-7289.

[17] L. Li, D. Quan, J. Chen, J. Ding, J. Zhao, L. Lv, J. Chen, Design, synthesis, and biological evaluation of 1-substituted -2-aryl imidazoles targeting tubulin polymerization as potential anticancer agents, European journal of medicinal chemistry, 184 (2019) 111732.

[18] C.-M. Li, J. Chen, Y. Lu, R. Narayanan, D.N. Parke, W. Li, S. Ahn, D.D. Miller, J.T. Dalton, Pharmacokinetic Optimization of 4-Substituted Methoxybenzoyl-aryl-thiazole and 2-Aryl-4-benzoyl-imidazole for Improving Oral Bioavailability, Drug Metabolism and Disposition, 39 (2011) 1833-1839.

[19] J. Chen, C.-M. Li, J. Wang, S. Ahn, Z. Wang, Y. Lu, J.T. Dalton, D.D. Miller, W. Li, Synthesis and antiproliferative activity of novel 2-aryl-4-benzoyl-imidazole derivatives targeting tubulin polymerization, Bioorgan Med Chem, 19 (2011) 4782-4795.

[20] Y. Lu, J. Chen, J. Wang, C.M. Li, S. Ahn, C.M. Barrett, J.T. Dalton, W. Li, D.D. Miller, Design, synthesis, and biological evaluation of stable colchicine binding site tubulin inhibitors as potential anticancer agents, Journal of medicinal chemistry, 57 (2014)

7355-7366.

[21] M.A. Zhai, S.Y. Liu, M.Q. Gao, L. Wang, J. Sun, J.A. Du, Q. Guan, K. Bao, D.Y. Zuo, Y.L. Wu, W.G. Zhang, 3,5-Diaryl-1H-pyrazolo[3,4-b]pyridines as potent tubulin polymerization inhibitors: Rational design, synthesis and biological evaluation, European journal of medicinal chemistry, 168 (2019) 426-435.

[22] J.B. Shi, W.J. Tang, X.B. qi, R. Li, X.H. Liu, Novel pyrazole-5-carboxamide and pyrazole–pyrimidine derivatives: Synthesis and anticancer activity, European journal of medicinal chemistry, 90 (2015) 889-896.

[23] S. Cherukupalli, R. Karpoormath, B. Chandrasekaran, G.A. Hampannavar, N. Thapliyal, V.N. Palakollu, An insight on synthetic and medicinal aspects of pyrazolo[1,5-a]pyrimidine scaffold, European journal of medicinal chemistry, 126 (2017) 298-352.

[24] L. Li, S. Jiang, X. Li, Y. Liu, J. Su, J. Chen, Recent advances in trimethoxyphenyl (TMP) based tubulin inhibitors targeting the colchicine binding site, European journal of medicinal chemistry, 151 (2018) 482-494.

[25] M.a. Zhai, L. Wang, S. Liu, L. Wang, P. Yan, J. Wang, J. Zhang, H. Guo, Q. Guan, K. Bao, Y. Wu, W. Zhang, Synthesis and biological evaluation of (1-aryl-1H-pyrazol-4-yl) (3,4,5-trimethoxyphenyl)methanone derivatives as tubulin inhibitors, European journal of medicinal chemistry, 156 (2018) 137-147.

[26] Z. Wang, J. Chen, J. Wang, S. Ahn, C.-M. Li, Y. Lu, V.S. Loveless, J.T. Dalton, D.D. Miller, W. Li, Novel Tubulin Polymerization Inhibitors Overcome Multidrug Resistance and Reduce Melanoma Lung Metastasis, Pharmaceutical research, 29 (2012) 3040-3052.

[27] Q. Wang, K. Arnst, Y. Wang, G.K. Kumar, D. Ma, S.W. White, D.D. Miller, W. Li, W. Li, Structure guided design, synthesis, and biological evaluation of 2-(1H-Indol-3-yl)-1H-imidazol-4-yl)(3,4,5-trimethoxyphenyl) Methanone (ABI-231) analogs targeting the colchicine binding site in tubulin, Journal of medicinal chemistry, 62 (2019) 6734 - 6750.

[28] K.E. Arnst, Y. Wang, D.-J. Hwang, Y. Xue, T. Costello, D. Hamilton, Q. Chen, J. Yang, F. Park, J.T. Dalton, D.D. Miller, W. Li, A Potent, Metabolically Stable Tubulin Inhibitor Targets the Colchicine Binding Site and Overcomes Taxane Resistance, Cancer research, 78 (2018) 265-277.

[29] K. Diederichs, P.A. Karplus, Improved R-factors for diffraction data analysis in macromolecular crystallography, Nature structural biology, 4 (1997) 269-275.

[30] P.A. Karplus, K. Diederichs, Linking crystallographic model and data quality, Science, 336 (2012) 1030-1033.

[31] S. Banerjee, K.E. Arnst, Y. Wang, G. Kumar, S. Deng, L. Yang, G.-b. Li, J. Yang, S.W. White, W. Li, D.D. Miller, Heterocyclic-Fused Pyrimidines as Novel Tubulin Polymerization Inhibitors Targeting the Colchicine Binding Site: Structural Basis and Antitumor Efficacy, Journal of medicinal chemistry, 61 (2018) 1704-1718.

[32] Q. Wang, K.E. Arnst, Y. Wang, G. Kumar, D. Ma, S.W. White, D.D. Miller, W. Li, W. Li, Structure-Guided Design, Synthesis, and Biological Evaluation of (2-(1H-Indol-3-yl)-1H-imidazol-4-yl)(3,4,5-trimethoxyphenyl) Methanone (ABI-231) Analogues Targeting the Colchicine Binding Site in Tubulin, Journal of medicinal chemistry, 62 (2019) 6734-6750.

[33] H. Chen, S. Deng, Y. Wang, N. Albadari, G. Kumar, D. Ma, W. Li, S.W. White, D.D. Miller, W. Li, Structure–Activity Relationship Study of Novel 6-Aryl-2-benzoyl-pyridines as Tubulin Polymerization Inhibitors with Potent Antiproliferative Properties, Journal of medicinal chemistry, 63 (2020) 827-846.

[34] E. Charbaut, P.A. Curmi, S. Ozon, S. Lachkar, V. Redeker, A. Sobel, Stathmin Family Proteins Display Specific Molecular and Tubulin Binding Properties, Journal of Biological Chemistry, 276 (2001) 16146-16154.

[35] A. Dorléans, B. Gigant, R.B.G. Ravelli, P. Mailliet, V. Mikol, M. Knossow, Variations in the colchicine-binding domain provide insight into the structural switch of tubulin, Proceedings of the National Academy of Sciences, 106 (2009) 13775-13779.

[36] Y. Wang, H. Zhang, B. Gigant, Y. Yu, Y. Wu, X. Chen, Q. Lai, Z. Yang, Q. Chen, J. Yang, Structures of a diverse set of colchicine binding site inhibitors in complex with tubulin provide a rationale for drug discovery, The FEBS Journal, 283 (2016) 102-111.

[37] Y. Wang, Y. Yu, G.-B. Li, S.-A. Li, C. Wu, B. Gigant, W. Qin, H. Chen, Y. Wu, Q. Chen, J. Yang, Mechanism of microtubule stabilization by taccalonolide AJ, Nature communications, 8 (2017) 15787.

[38] A.E. Prota, K. Bargsten, D. Zurwerra, J.J. Field, J.F. Diaz, K.-H. Altmann, M.O. Steinmetz, Molecular Mechanism of Action of Microtubule-Stabilizing Anticancer Agents, Science, 339 (2013) 587-590.

[39] Z. Otwinowski, W. Minor, [20] Processing of X-ray diffraction data collected in oscillation mode, Methods in Enzymology, 276 (1997) 307-326.

[40] P.D. Adams, R.W. Grosse-Kunstleve, L.-W. Hung, T.R. Ioerger, A.J. McCoy, N.W. Moriarty, R.J. Read, J.C. Sacchettini, N.K. Sauter, T.C. Terwilliger, PHENIX: building new software for automated crystallographic structure determination, Acta Crystallographica Section D, 58 (2002) 1948-1954.

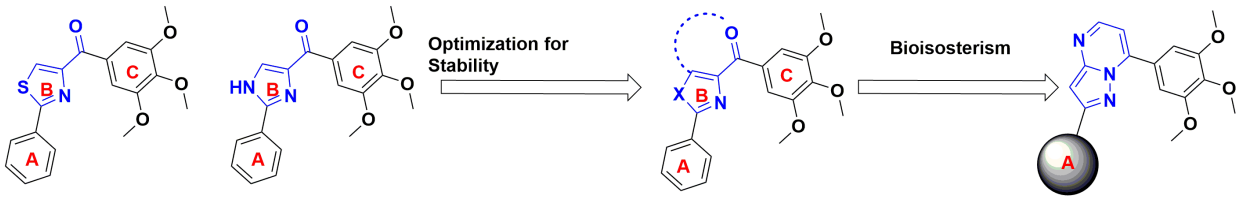

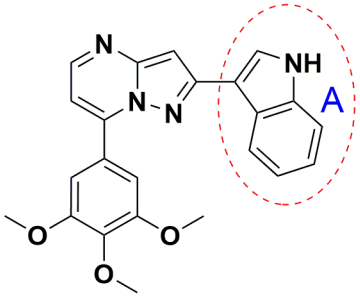

1aa

"Bent" conformation

IC_{50} = 76.8 nM

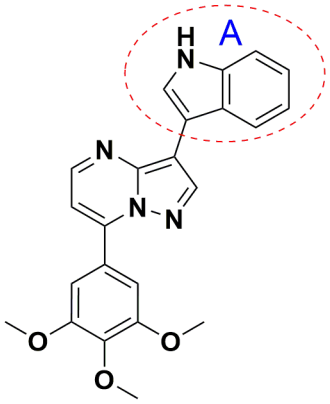

7

"Straight" conformation

IC_{50} > 10 μM

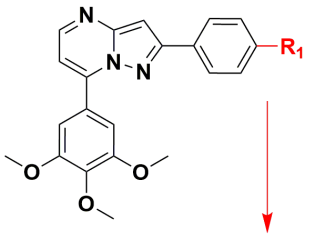

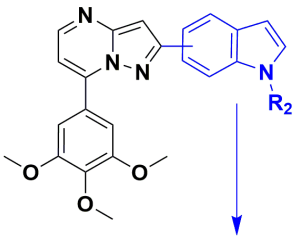

Substitutions at C-4 of benzene (R_1): CH_3 is optimal; CH_3 > EDG > H > EWG

Substitutions at N-1 of indole (R_2): H > methylol > methyl
Substitution at C-5 position of indole is the best

EDG: electron-donating group
EWG: electron-withdrawing group

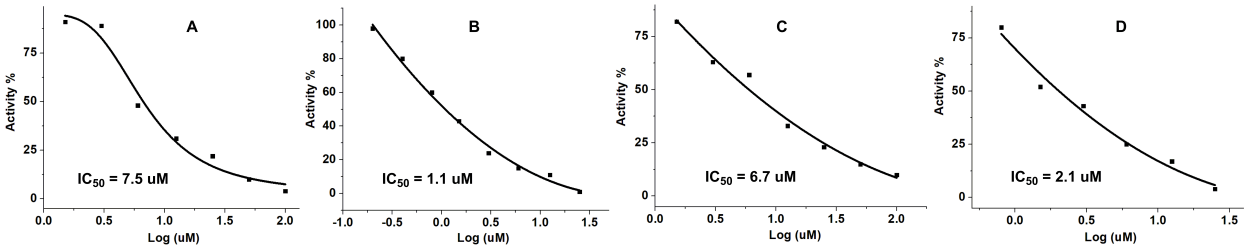

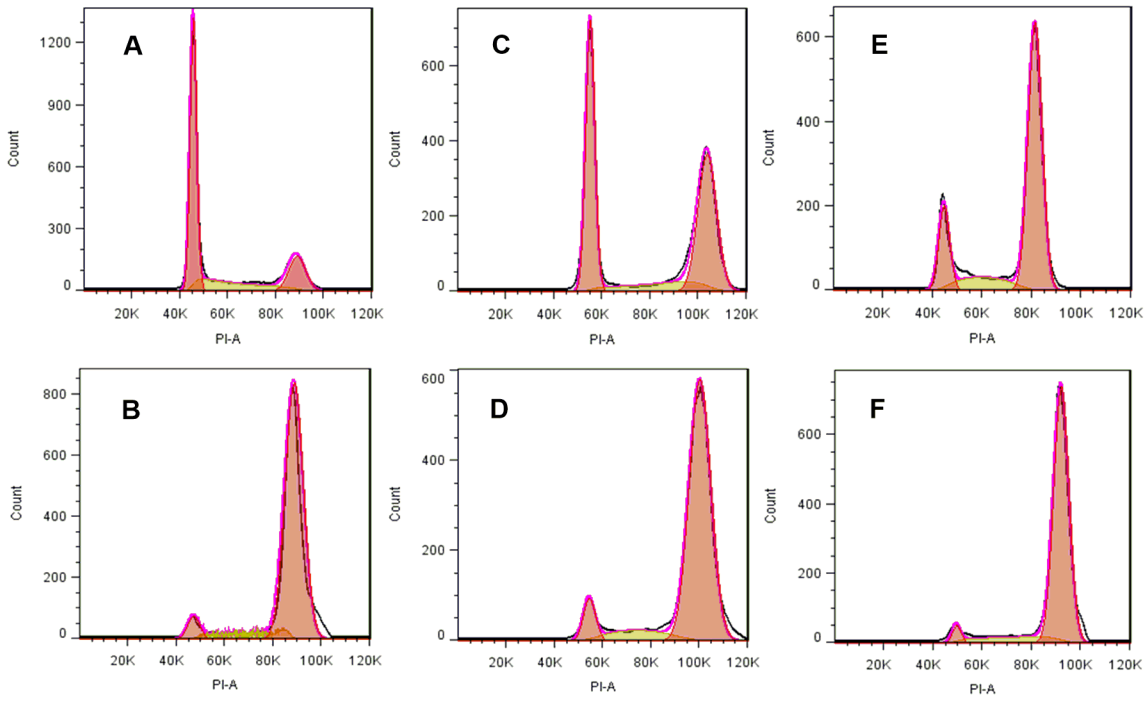

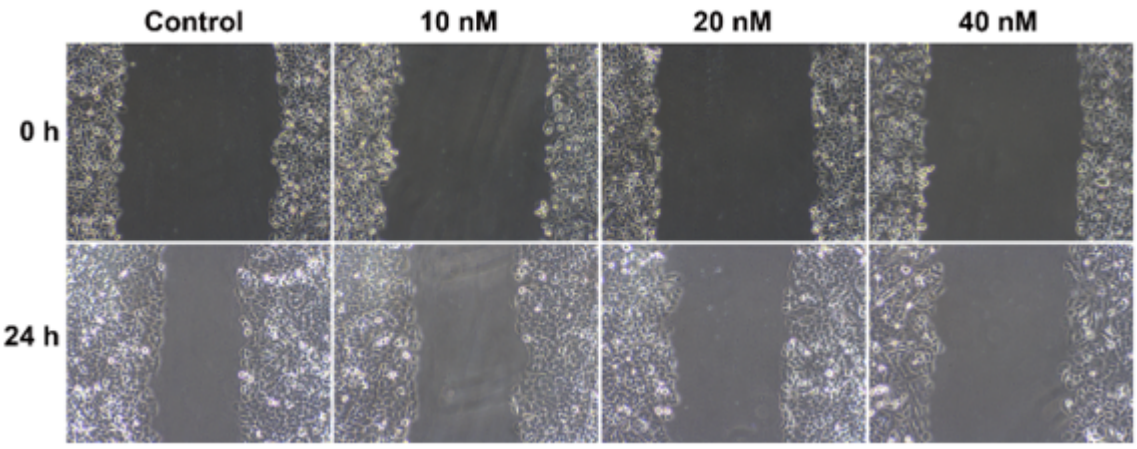

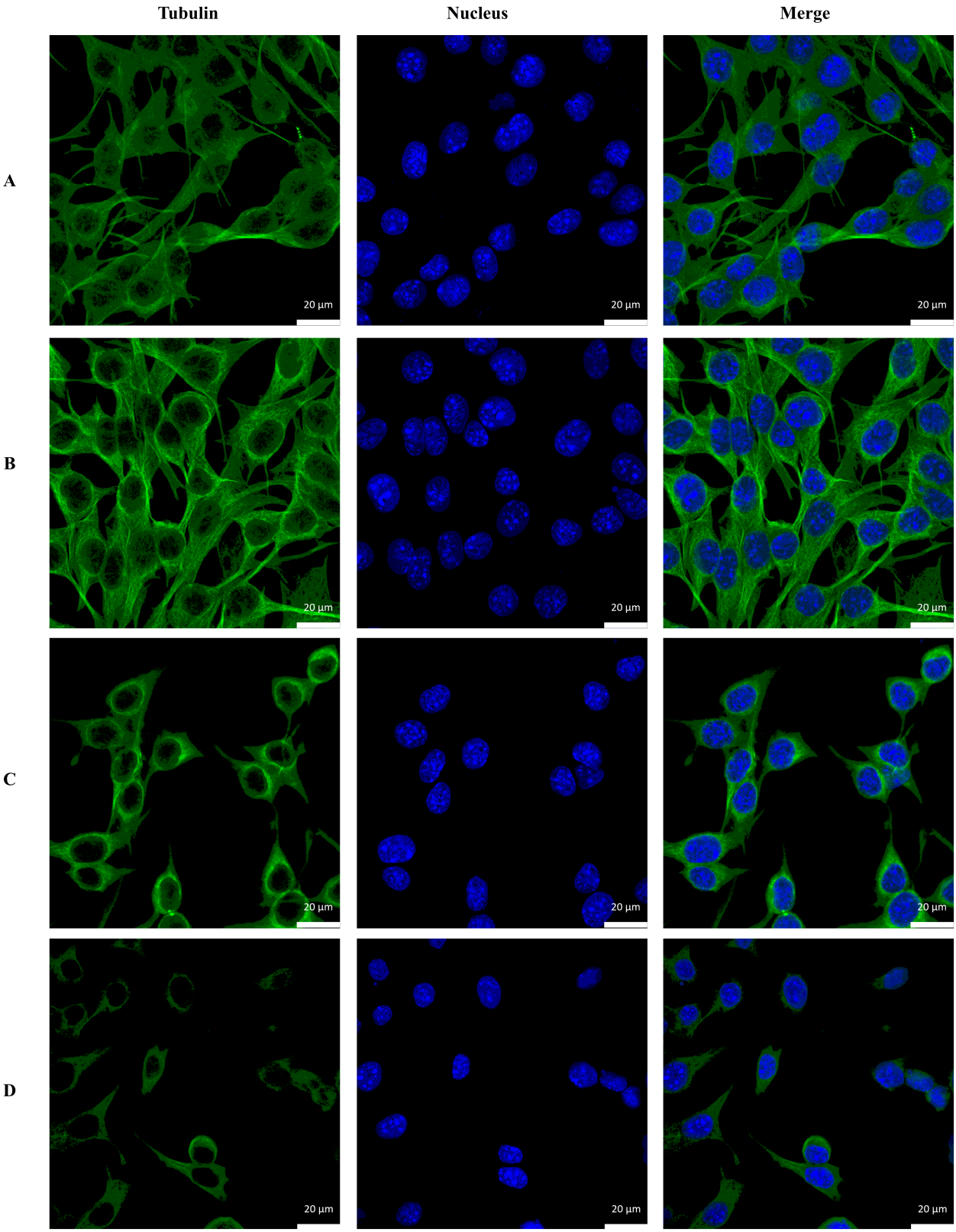
Tubulin
Nucleus
Merge
A
B
C
D
20 μm

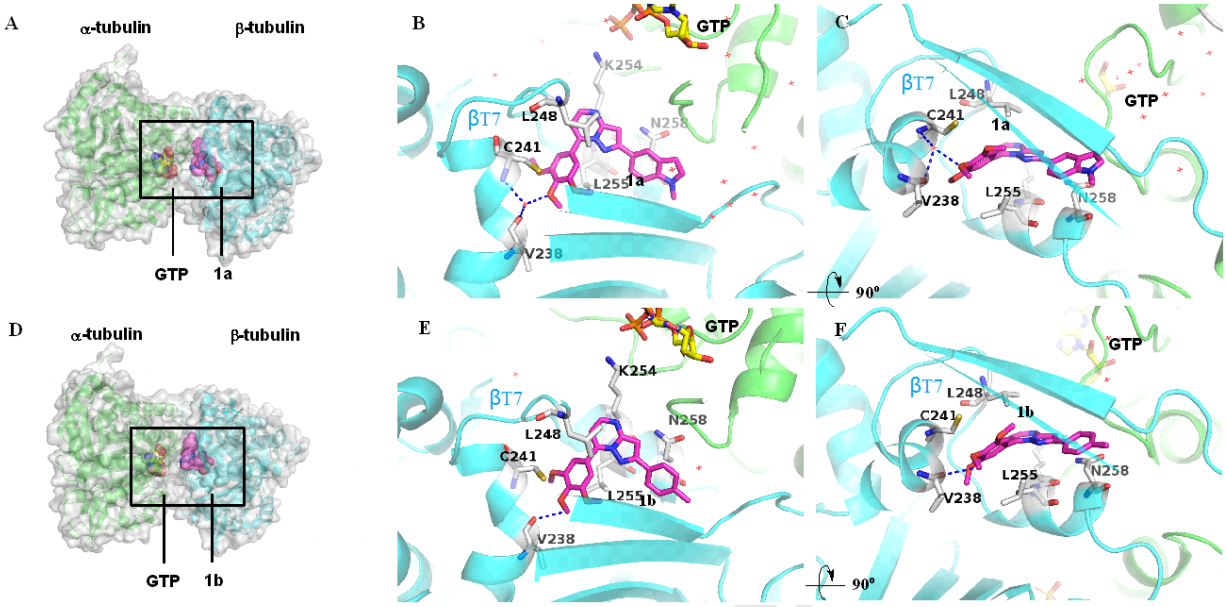

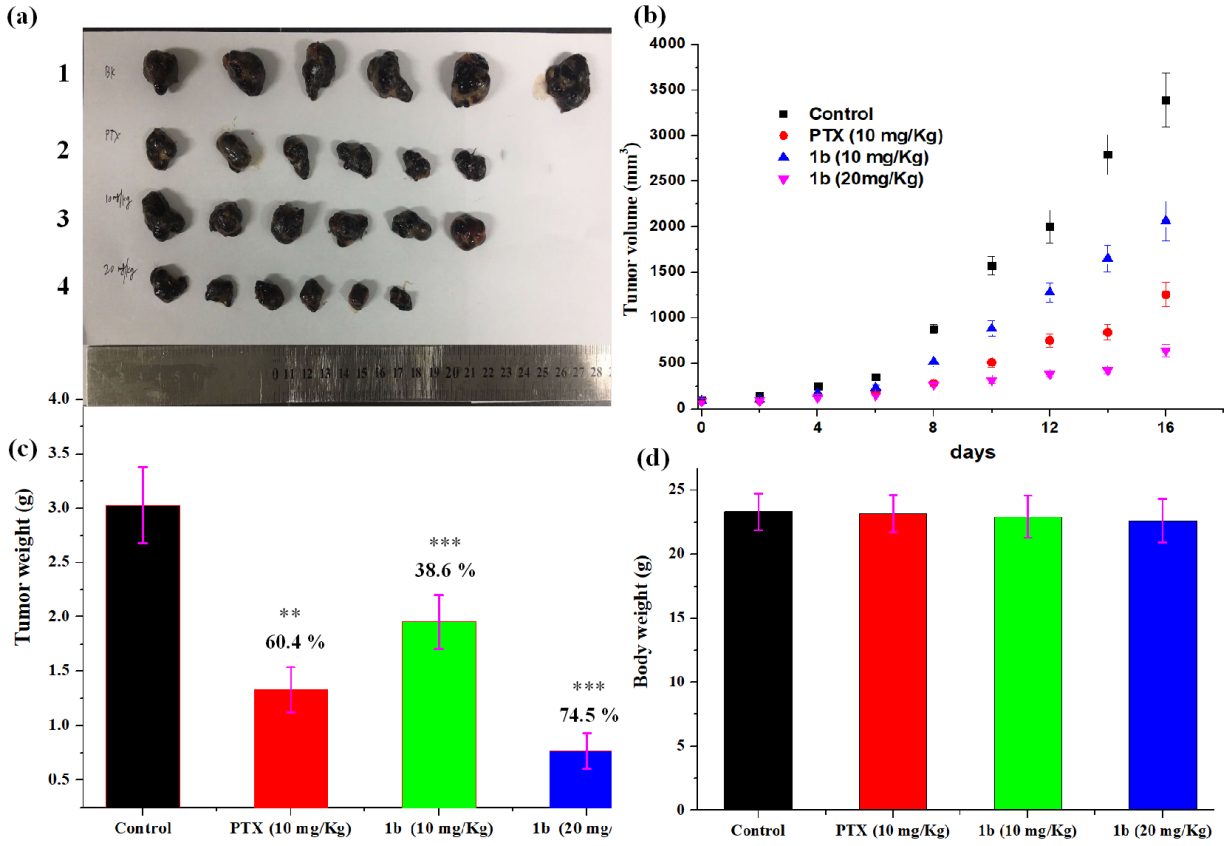
(a)
1
2
3
4
(b)
Tumor volume (mm3)
Control
PTX (10 mg/Kg)
1b (10 mg/Kg)
1b (20mg/Kg)
days
(c)
Tumor weight (g)
**
60.4 %
***
38.6 %
***
74.5 %
Control
PTX (10 mg/Kg)
1b (10 mg/Kg)
1b (20 mg/
(d)
Body weight (g)
Control
PTX (10 mg/Kg)
1b (10 mg/Kg)
1b (20 mg/Kg)

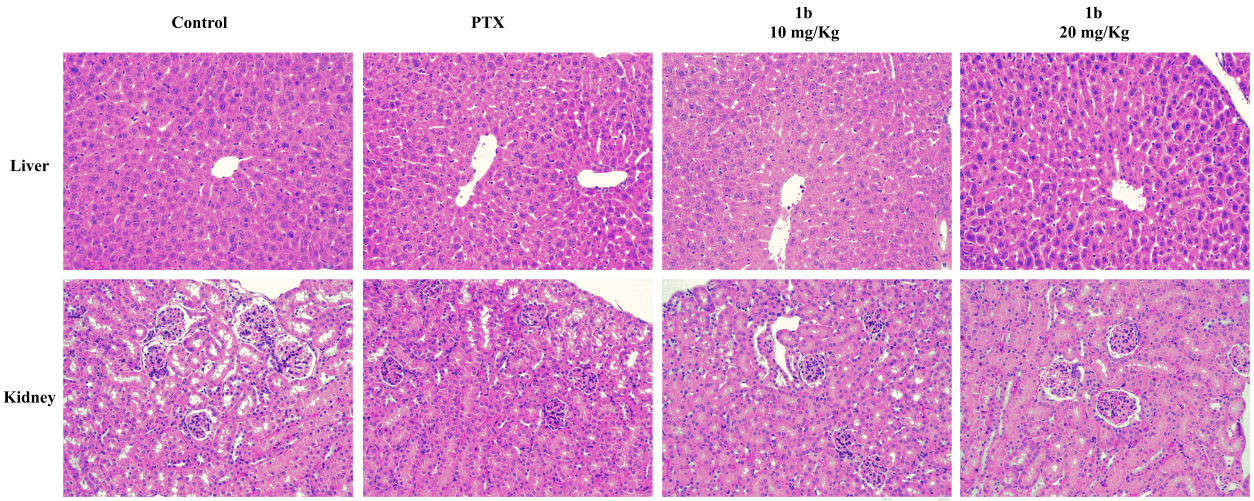

Highlights

- Pyrazolo[1,5-a]Pyrimidine analogs were discovered as novel tubulin inhibitors
- **1b** displayed high antiproliferative activity with IC_{50} of 28 nM
- Crystal structures of **1a** and **1b** in complex with tubulin were solved
- **1b** exhibited high metabolic stability in liver microsomes ($T_{1/2}$ ⩾120 min)
- **1b** showed high in vivo antitumor efficacy in a B16-F10 mouse melanoma model

Declaration of interests

☒ The authors declare that they have no known competing financial interests or personal relationships that could have appeared to influence the work reported in this paper.

☐The authors declare the following financial interests/personal relationships which may be considered as potential competing interests: